ISTANBUL TECHNICAL UNIVERSITY ★ GRADUATE SCHOOL

EXPERIMENTAL INVESTIGATION OF BOUNDARY LAYER TRANSITION VIA VORTEX GENERATORS

M.Sc. THESIS

İsmet Cihat AY

Department of Defense Technologies

Defense Technologies Programme

JUNE 2023

ISTANBUL TECHNICAL UNIVERSITY ★ GRADUATE SCHOOL

EXPERIMENTAL INVESTIGATION OF BOUNDARY LAYER TRANSITION VIA VORTEX GENERATORS

M.Sc. THESIS

İsmet Cihat AY
(514191053)

Department of Defense Technologies

Defense Technologies Programme

Thesis Advisor: Dr. Duygu ERDEM

JUNE 2023

İSTANBUL TEKNİK ÜNİVERSİTESİ ★ LİSANSÜSTÜ EĞİTİM ENSTİTÜSÜ

VORTEKS ÜRETEÇLERİ İLE SINIR TABAKADAKİ AKIŞIN LAMİNERDEN TÜRBÜLANSA GEÇİŞİNİN DENEYSEL İNCELENMESİ

YÜKSEK LİSANS TEZİ

İsmet Cihat AY
(514191053)

Savunma Teknolojileri Anabilim Dalı

Savunma Teknolojileri Programı

Tez Danışmanı: Dr. Duygu ERDEM

HAZİRAN 2023

İsmet Cihat AY, a M.Sc. student of ITU Graduate School student ID 514191053 successfully defended the thesis entitled "EXPERIMENTAL INVESTIGATION OF BOUNDARY LAYER TRANSITION VIA VORTEX GENERATORS", which he/she prepared after fulfilling the requirements specified in the associated legislations, before the jury whose signatures are below.

Thesis Advisor :	**Dr. Duygu ERDEM** Istanbul Technical University	.....
Jury Members :	**Doç. Dr. Sertaç ÇADIRCI** Istanbul Technical University	.....
	Prof. Dr. A. Cihat BAYTAŞ Istanbul Technical University	.....
		.....

Date of Submission : **26 May 2023**
Date of Defense : **04 July 2023**

To my family,

FOREWORD

First and foremost, I would like to express my gratitude to my advisor, Dr. Duygu Erdem who gave me the great opportunity to be the part of a research project. She was always supportive and considerate. Being her student and studying under guidance was one of the greatest experience in my life. I am really grateful for the opportunities both personally and academically.

I would also like to thank my closest friends; Burakhan Şüküroğlu, Osman Giray Oğuzman and Onur Yasin Yüceer for their support and friendship during the hard times. Their priceless companionship has brought me to the end.

My special thanks goes to my dearest parents, my mother Neslihan Ay, my father Abdullah Ay, my brother Elvan Batuhan Ay and my sisters. I have been constantly supported and encouraged even at the times when I did not believe in myself. Last couple of days were extremely challenging for us. Unconditional supports through my whole life aside, I will never be thankful enough for your efforts to make me focus on my study alone for these days.

HAZİRAN 2023

İsmet Cihat AY
M.Sc Student

TABLE OF CONTENTS

ABBREVIATIONS

App : Appendix
St : Station
VGs : Vortex Generators
MVG : Miniature Vortex Generator
PG : Pressure Gradient
TS : Tollmien-Schlichting
IB : immersed boundary
MTL : minimum turbulence level
KARI : Korea Aerospace Research Institute
DNSs : Direct numerical simulations
CCA : Constant Current Anemometer
CTA : Constant Temperature Anemometer
AF10 : Air flow bench
KTH : Royal Institute of Technology
2D : two-dimensional
3D : three-dimensional
BL : Boundary Layer

SYMBOLS

t	**:** Time
u	**:** mean velocity
U	**:** Free-stream velocity
Re	**:** Reynolds number
x	**:** position
δ	**:** Boundary layer thickness
δ^*	**:** Displacement thickness
θ	**:** Momentum thickness
$\frac{\partial P}{\partial x}$	**:** Pressure Gradient

LIST OF TABLES

Page

LIST OF FIGURES

EXPERIMENTAL INVESTIGATION OF BOUNDARY LAYER TRANSITION VIA VORTEX GENERATORS

SUMMARY

The structure and properties of the flow is an extremely important issue for engineers and system designers working on a flow system. Knowing the flow details in the boundary layer of many structures in aviation technology is important for solving many problems in aerodynamics. These problems are skin friction drag of an object, the development of a wing stall, the heat transfer that occurs in high velocity flight, and the performance of a high velocity airplane entry. An object's boundary layer begins as laminar, and when the critical angle of attack is exceeded in aircraft wings, the airflow becomes turbulent and the lift decreases rapidly. Free stream turbulence and pressure gradient are thought to be the most effective parameters in boundary layer transition from laminar state to turbulent state.

There are many passive and active control methods to prevent or delay the transition in the boundary layer, one of them is vortex generators. Vortex Generators have a mechanism that prevents or delays boundary layer separations under the effect of reverse pressure gradient by increasing the energy of the boundary layer with the vortices they produce. The vortex generator increases the energy level of the layer by transporting energy from the outer flow to the boundary layer, thereby increasing the performance of many vehicles. Vortex generators are frequently used in the aerodynamic design of many land and aircraft because they can significantly prevent flow separation. Vortex generators are a common flow tool, especially in aviation technology, because they improve flow characteristics and most importantly save energy.

In this thesis, the transition from laminar to turbulent flow in the boundary layer by means of vortex generators is experimentally investigated. The purpose of using vortex generators in this study is to explain in detail how they affect the flow in the boundary layer. Within the scope of the thesis, first of all, literature research was carried out about the vortex generators and the transition from laminar to turbulent flow in the boundary layer. In line with the researches, a spherical ball with a diameter of 1 mm was chosen as the vortex generator.

The studies were carried out in the Trisonic Research Laboratory of the Faculty of Aeronautics and Astronautics of Istanbul Technical University. Experiments were carried out on a modular air flow bench (AF10) experimental setup using a 27 cm long brass flat plate. AF10 consists of a small scale wind tunnel with adjustable airflow control and an electric fan. A flattened Pitot tube measures the total pressure at various distances from the plate surface by positioning the Pitot tube using a micrometer. The results are obtained by connecting the Pitot tube to the Setra brand model 239 pressure

transducer. This transducer response time is lower than 10ms. During data acquisition mean value of 10000 data is used for each measurement point.

Additionally, A hot wire anemometer was used for velocity measurements, another experimental setup. Dantec StreamLine system was used for speed measurement. The 55P15 boundary layer type probe was used in the study. This probe is a constant temperature probe designed for use in boundary layers and is used via a probe support. The probe needs to be calibrated prior to experiments. Velocity profiles were measured at various locations on the surface.

Experiments with and without a vortex generator were performed and the boundary layer flow under investigation was subjected to a positive pressure gradient and these experiments were compared. Experiments were carried out for 10 different ratios in the range of vortex generator height divided by boundary layer thickness, that is, the ratio h/δ, between 0.4 and 0.8. According to the results of the experiments for flow velocities 8,9,10,12 and 15 m/s without the vortex generator, it was determined that the flow in the boundary layer is laminar since the boundary layer thickness values found overlap with the Blasius solution in many locations.

After positioning the vortex generators, it was determined that the flow of VGs kept the flow laminar for 4 or 5 cm and then the flow transitioned. It was determined that the positive pressure gradient effect increased the boundary layer thickness in the experiments. It was also found that this effect makes the flow turbulent faster in experiments with vortex generators.Finally, where the vortex generators will be placed on the plate is a very important issue which determines transition onset and transition length.

VORTEKS ÜRETEÇLERİ İLE SINIR TABAKADAKİ AKIŞIN LAMİNERDEN TÜRBÜLANSA GEÇİŞİNİN DENEYSEL İNCELENMESİ

ÖZET

Akışın yapısı ve özellikleri, bir akış sistemi üzerinde çalışan mühendisler ve sistem tasarımcıları için son derece önemli bir konudur. Havacılık teknolojisindeki birçok yapının sınır tabakasındaki akış detaylarının bilinmesi, aerodinamikteki birçok problemin çözümü için önemlidir. Bu problemler, bir cismin yüzey sürtünme direnci, kanat stall gelişimi, yüksek hızlı uçuşta meydana gelen ısı transferi ve yüksek hızlı uçak girişinin performansıdır. Bir cismin sınır tabakası laminer olarak başlar ve uçak kanatlarında kritik hücum açısı aşıldığında hava akımı türbülanslı hale gelir ve kaldırma kuvveti hızla düşer. Serbest akış türbülansı ve basınç gradyanının, sınır tabakadaki akışın laminer durumdan türbülanslı duruma geçişinde en etkili parametreler olduğu düşünülmektedir.

Sınır tabakasındaki geçişi önlemek veya geciktirmek için birçok pasif ve aktif kontrol yöntemi vardır, bunlardan biri de girdap üreteçleridir. Girdap üreteçleri, ürettikleri girdaplar ile sınır tabakasının enerjisini arttırarak, ters basınç gradyanının etkisi altında olan sınır tabakası ayrılmalarını engelleyen veya geciktiren bir mekanizmaya sahiptir. Girdap üreteci, dış akıştan sınır tabakaya enerji taşıyarak tabakanın enerji seviyesini yükseltir ve böylece birçok aracın performansını artırır. Girdap üreteçleri, akış ayrılmasını önemli ölçüde önleyebildikleri için birçok araç ve uçağın aerodinamik tasarımında sıklıkla kullanılmaktadır. Girdap üreteçleri, akış özelliklerini iyileştirdikleri ve en önemlisi enerji tasarrufu yaptıkları için özellikle havacılık teknolojisinde yaygın bir akış aracıdır.

Bu tezde, sınır tabakasındaki akış laminer akıştan türbülanslı akışa geçerken girdap üreteçleri aracılığıyla deneysel olarak incelenmiştir. Bu çalışmada girdap üreteçlerinin kullanılmasının amacı, sınır tabakasındaki akışı nasıl etkilediklerini detaylı olarak açıklamaktır. Tez kapsamında öncelikle girdap üreteçleri ve sınır tabakasındaki akışın laminer akıştan türbülanslı akışa geçişi ile ilgili literatür araştırması yapılmıştır. Yapılan araştırmalar doğrultusunda girdap üreteci olarak 1 mm çapında küresel bir top seçilmiştir.

Çalışmalar, İstanbul Teknik Üniversitesi, Uçak ve Uzay Bilimleri Fakültesi Trisonik araştırma laboratuvarında gerçekleştirildi. Deneyler, 27 cm uzunluğundaki pirinç düz bir plaka kullanılarak modüler bir hava akışı masası olan deney düzeneği üzerinde gerçekleştirildi. Hava akış masası, ayarlanabilir hava akışı kontrolüne ve bir elektrikli fana sahip küçük ölçekli bir rüzgar tünelinden oluşur. Ünite, üzerine aerodinamik olarak şekillendirilmiş konstrüksiyona hava sağlayan bir fanın ve bir akış kontrol valfi aracılığıyla özel olarak tasarlanmış bir plenum odasının monte edildiği sağlam bir çelik çerçeveden oluşur. Test modüllerini tutmak için mafsallı kıskaçlar ve basınç ölçüm

bağlantıları için güvenilir hızlı açılan kaplinler kullanılır. Bu iki özellik sayesinde bir deneyden diğerine geçmek basit ve hızlıdır.

Bir mikrometre ile konumlandırılmış düzleştirilmiş bir Pitot tüpü ile plaka yüzeyinden çeşitli mesafelerdeki toplam basınç ve dolayısıyla hız ölçülür. Pitot tüpü, hızlı bağlama-çözme kaplini ile donatılmış esnek bir tüp aracılığıyla bir basınç dönüştürücüye bağlanır. Setra marka Model 239 basınç transdüseri kullanılmıştır. Model 239, -18 ila 80 °C sıcaklık aralığında ±0,073% FS doğruluğu ile çeşitli basınç aralıklarını kapsar. Ayrıca dönüştürücünün tepki süresi 10 milisaniyeden düşüktür. Veri toplama sırasında her bir ölçüm noktası için ortalama 10000 veri değeri kullanılır.

Ek olarak, hız ölçümleri için bir başka deney düzeneği olan sıcak telli bir anemometre kullanıldı. Sabit sıcaklık anemometresi, bir noktadaki hızın zamana göre değişimini verir. Böylece yoğunluk ve zamana bağlı istatistikler yapılabilmektedir. Bunun örnekleri, ortalama hız, türbülans yoğunluğu, yüksek dereceli momentler, oto-korelasyon ve güç spektrumudur. Hız ölçümü için Dantec StreamLine sistemi kullanılmıştır. Dantec Dynamics, sabit sıcaklık anemometreleri ile kullanım için eksiksiz bir prob sistemi sunar ve türbülanslı gaz ve sıvı akışlarındaki mikro yapıların ölçümü ve analizi için günümüzde en yaygın kullanılan araçtır. Sabit sıcaklık anemometresi prob programı, çeşitli prob tiplerini ve prob konfigürasyonlarını içerir. Çalışmada 55P15 sınır tabaka tipi prob kullanılmıştır. Bu prob, sınır katmanlarında kullanılmak üzere tasarlanmış sabit bir sıcaklık probudur ve bir prob desteği ile kullanılır. Prob desteği bir ara bağlantının üzerine yerleştirilir ve hız profillerini belirlemek için verilen koordinatlar doğrultusunda hareket eder. Hız profilleri, yüzeydeki çeşitli konumlarda ölçülmüştür. Probun deneylerden önce kalibre edilmesi gerekir. Amaç, sabit sıcaklık anemometresi çıkış voltajıyla bilinen akış hızları arasındaki ilişkiyi belirlemektir. Kalibrasyon ünitesi, sabit sıcaklık anemometre sistemleriyle kullanılan çoğu sıcak tel probu için oldukça hassas bir araçtır. Sıcak tel kalibratörü serbest bir jet üretir ve kalibrasyon sırasında prob bu jetin içindedir. Basınçlı hava gereklidir ve bu sistem ile 0,5 m/s ile 300 m/s arasındaki hızlar ayarlanabilmektedir. Kalibrasyon eğrisi ile veriler arasındaki hata, tüm kalibrasyonlar için yüzde 1'den azdır.

Bu tezde sabit sıcaklık sınır koşulu altında sınır tabakasındaki akışın değişimi incelenmiştir. Sınır tabakasındaki akışın laminerden türbülansa geçtiği konumları belirlemek için deneyler yapılmış ve girdap oluşturucunun bu duruma etkisi incelenmiştir. Bu çalışmada ilk önce plaka için farklı akış hızlarında farklı aşağı akış konumlarında deneyler yapılmıştır. Daha sonra üzerine girdap oluşturucu yerleştirildi ve farklı parametrelerle asıl deneylere başlandı. Deneylerde parametre olarak serbest akış hızı ve girdap üreteci konumu kullanılmıştır. Ayrıca deney düzeneğine basınç gradyanı oluşturmak için parçalar eklenerek deneyler yapılmıştır. Yapılan bu girdap üreteçli, girdap üreteçsiz, basınç gradyenli ve basınç gradyensiz bütün deneyler karşılaştırılıp sonuçlara ulaşılmıştır. Deneyler, girdap üreteci yüksekliğinin sınır tabakası kalınlığına bölünmesi, yani h/δ oranı, 0,4 ile 0,8 aralığında 10 farklı oran için gerçekleştirilmiştir.

Girdap üreteci olmadan 8,9,10,12 ve 15 m/s akış hızları için yapılan deneylerin sonuçlarına göre, bulunan sınır tabaka kalınlık değerleri birçok konumda Blasius'un teorik değerleriyle örtüştüğü için sınır tabakadaki akışın laminer olduğu belirlenmiştir.

Ayrıca girdap üreteci kullanılmadan yapılan deneylerin sonuçları delta (δ) ve Reynold sayısı grafikleri çizilerek doğrulanmıştır. Yapılan deneylerde pozitif basınç gradyan etkisinin sınır tabaka kalınlığını arttırdığı belirlenmiştir.

Girdap üreteçleri konumlandırıldıktan sonra girdap üreteçlerinin sınır tabakadaki akışı 4 veya 5 cm kadar laminer tuttuğu ve daha sonra akışın geçiş yaptığı belirlendi. Girdap üreteçleri ile yapılan deneylerde bu etkinin akışı daha hızlı çalkantılı hale getirdiği de bulundu. Ayrıca girdap üreteçleri ile yapılan deneylerde sınır tabakadaki geçiş bölgesi uzunluğunun girdap üreteçleri ile azaldığı tespit edilmiştir. Son olarak girdap üreteçlerinin plaka üzerinde nereye yerleştirileceği de geçiş başlangıcını ve geçiş uzunluğunu belirleyen çok önemli bir konudur.

1. INTRODUCTION

One of the methods frequently used to increase the performance of many vehicles, which are considered in terms of hydrodynamics and aerodynamics, is vortex generators. Vortex generators were first studied in the late 1940s for the purpose of controlling (delaying) separation in aircraft wings and wind tunnels, and were found to be very useful. Vortex generators are most commonly used to prevent flow separation. If the boundary layer on a lifting surface is laminar, flow separation may occur at an earlier stage, resulting in stall at low angles of attack. Vortex generators can be used to prevent this phenomenon. Vortex generators have many different application areas, one of them being used in high performance cars to reduce drag. In addition, vortex generators can control flow separation when used in wind turbine blades, thereby improving turbine power output.

Since the flow separation event causes great energy losses, it directly affects the performances of many air, land and sea vehicles in terms of hydrodynamics and aerodynamics. Flow separation occurs as a result of the adverse pressure gradient. This phenomenon creates many undesirable effects such as an increase in drag force and a decrease in the magnitude of lift force. Flow separation also causes extra fuel consumption due to large energy losses. Various approaches have been developed on the control of this phenomenon. The common denominator of the approaches developed on the control of flow separations is to preserve the boundary layer attached on the surface as much as possible. Various flow separation control tools have been developed based on many methods and applications to maintain the boundary layer attached on the surface. Some of these methods are suction applications, form optimizations, vortex generators and wall heat transfer method [10].

With the vortex generators, which are frequently used in the aerodynamic design of land and air vehicles, the phenomenon of flow separation can be prevented to a significant extent. Easy to manufacture and implement, low-cost vortex generators

are available in the literature as flow instruments with simple geometries. Vortex generators induce extra momentum in the boundary layer, thereby increasing the boundary layer energy level, and this is achieved by the eddies they produce in the flow direction [6]. As a result, it becomes possible to prevent or delay separation with vortex generators. Vortex generators are a common flow tool, especially in aviation technology, because they improve flow characteristics and most importantly save energy. Vortex generators were primarily used in military aircraft and airline transport, and have since been used in general aviation as well. Vortex generators are mounted in aircraft on the leading edges of wings and on the horizontal stabilizers. In all airplanes, whether single-engine airplane or multi-engine airplane, vortex generators increase controllability at slow air speeds and reduce stall speeds. In addition, vortex generators can increase the useful load by providing a slower stall speed and a higher take-off weight in aircraft. One of the most important features of vortex generators is that they can keep the flow in the boundary layer laminar. Researchers have proven this in their work in the wind tunnel at the Royal Institute of Technology (KTH) in Stockholm [11]. This study was carried out under certain flow conditions by connecting miniature vortex generators to a flat plate.

1.1 Boundary Layer Transition

The structure and properties of the flow is an extremely important issue for engineers and system designers working on a flow system. Generally, flow can be classified as laminar or turbulent, and there is a phase in which the flow changes from laminar to turbulent but does not fully exhibit either flow behaviour. This is called the transition phase of the flow. Laminar flow promotes streamlined and parallel layer flow, and this flow is associated with Low Re number. When the Re number increases by a certain rate, the flow becomes turbulent and deviates from its aerodynamic path. The flow state between laminar and turbulent is considered a transitional flow, which can start at an arbitrary point during the flow. Reynolds number can be mathematically expressed as:

$$Re \equiv \frac{uL}{v} = \frac{\rho uL}{\mu} \tag{1.1}$$

ρ is the density of the fluid (SI units: kg/m3)

u is the flow speed (m/s)

L is a characteristic linear dimension (m)

μ is the dynamic viscosity of the fluid (Pa·s or N·s/m2 or kg/(m·s))

v is the kinematic viscosity of the fluid (m2/s).

Boundary layers can be laminar or turbulent (irregular) based on the value of the Local Re number. For lower Reynolds numbers, the boundary layer is laminar and the velocity in the flow direction changes smoothly with distance from the wall, as shown on the left side of the Figure 1.1. For higher Reynolds numbers, the boundary layer is turbulent and the velocity stream-wise is characterized by unstable (time varying) eddy flows within the boundary layer. Instability can be observed from the point where the transition Reynolds number (Re) is greater than 500,000 [1]. The stages of the formation of the boundary layer are shown in the figure below:

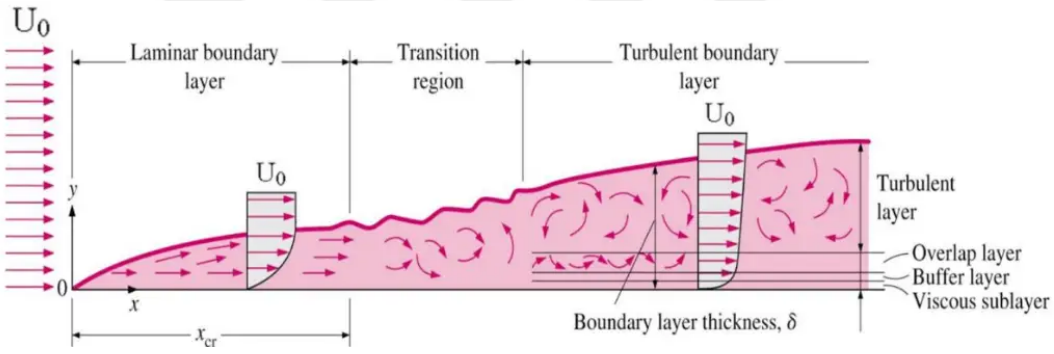

Figure 1.1 : Stages of formation of the boundary layer [1].

Additionally, it is known that the boundary layer transition from the laminar state to the turbulent state is affected by many parameters. Among these parameters, free stream turbulence and pressure gradient are considered to be the most effective.

1.2 Vortex Generator

Vortex Generators have a mechanism that prevents or delays boundary layer separations under the effect of reverse pressure gradient by increasing the energy of the boundary layer with the eddies they produce. In addition, vortex generators are used for other purposes. Some of these purposes include preventing flow in the boundary

layer from transitioning to early turbulent flow, reducing friction and increasing lift force. Lin's 2002 work contains extensive terminology information about vortex generators types, parameters and referenced studies as well as vortex generators. Various shapes have been presented for vortex generators that control flow separations [12]. Among these, flat plate type swirl makers, Wheeler wishbone, Wheeler doublet, backward-facing ramp and wedge types are among the most frequently used ones. Vortex generators are divided into two types according to their profile heights. These are conventional and low profile vortex generators. The profile heights of the vortex generators are expressed as h/δ according to the boundary layer thickness δ order. While the h/δ ratio of profile heights is about 1 in conventional vortex generators, the h/δ ratio is between 0.1 and 0.5 in low profile vortex generators. While the eddies produced by conventional VGs are stronger than those of low profile VGs, low profile VGs cause lower parasitic resistances.

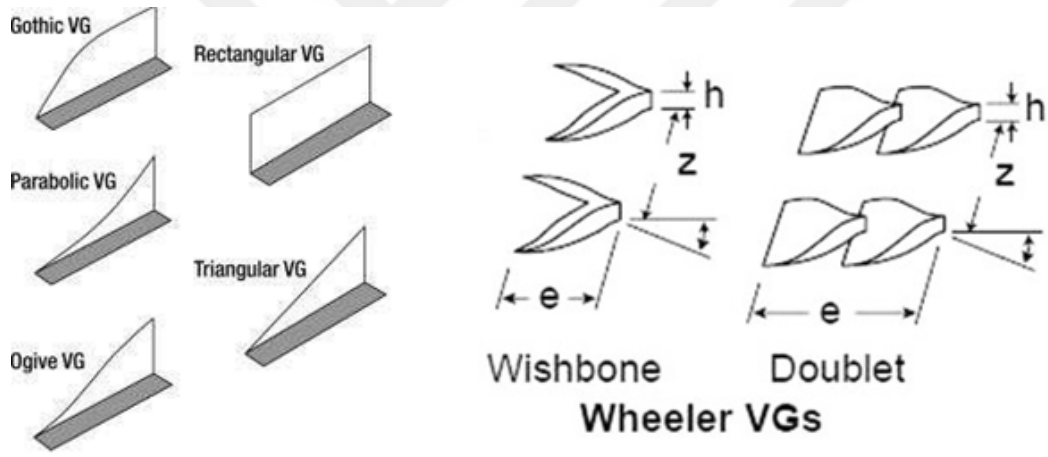

Figure 1.2 : Flat plate type VGs, Wheeler wishbone, Wheeler doublet VGs [2].

In addition, vortex generators are divided into two types according to the direction of rotation of the eddies they produce. These are co-rotational and counter-rotational vortex generators. While vortex generators with co-rotation eddy configurations are positioned in parallel, as the name suggests, produce eddies that rotate in the same direction as each other, while counter-rotation vortex generators are positioned opposite each other with their angles of attack to regulate the current by producing eddy pairs in opposite directions relative to each other.

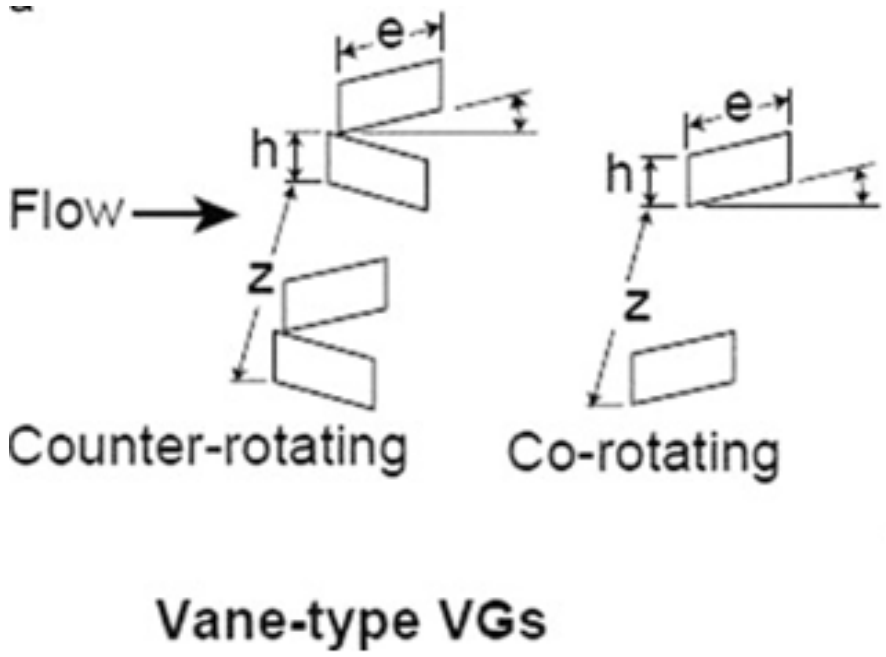

Figure 1.3 : Co-rotational and counter-rotational VGs [2].

1.3 Literature Review

In this study, vortex generators and the transition from laminar to turbulent flow in the boundary layer are considered as the main points and these are included in the literature review section. Many studies have been conducted on these issues and one of the studies was done by Itıro Tanı et al. in 1962. In this study, boundary layer transition was investigated in the presence of flow-through vortices [3]. Using the linearized laminar instability theory, it is assumed that the disturbances varieties occur before the transition in the boundary layer, since all sources of disturbance are also small. If the disturbance is not weak at the beginning, it starts to deviate from the theoretical prediction after a distance downstream, and that proves to be a non-linear effect before the flow begins to transition. The most striking feature of this effect is that although the initial distortion was purely two-dimensional, the distortions turned into a three-dimensional configuration. The formation of three-dimensional distortions along a flat plate is important so that the flow in the boundary layer can become turbulent and provides evidence for the presence of vortices with their axes downstream. The importance of downstream vortices in causing disruption of the

mean flow is considered to be related to boundary layer crossing caused by an isolated roughness element.

In this study, the results of an experimental investigation of instability leading to transition in subsonic boundary layer flow across a flat plate are presented. The experiments were carried out in a 20 by 60 cm low turbulence wind tunnel without pressure gradient effects on the boundary layer of a flat aluminum plate 300 cm long, 60 cm wide and 5 mm thick. The streamwise vortices were produced downstream by a series of wings placed outside the boundary layer, causing the boundary layer to be of periodic thickness. The wave or disturbance was created using the vibrating ribbon, and hot wire measurements were made to monitor the downstream evolution of the intensity and phase of this wave. The distributions of wave phase and wave intensity are different in different longitudinal sections. Linear development behaviour is that said to be proportional to the intensity distribution, independent of the phase distribution, as long as the initial distortion is weak. The distortion is first magnified but eventually fades as long as its intensity remains small. The reason why the wave development deviates from the linear development is that the excitation current is increased above a certain limit. This is done so that the initial distortion is no longer weak. The occurrence of non-linearity development causes disruption of laminar flow and thus the initiation of turbulence. This development occurs with the distortion in the mean velocity profile and the rapid increase in fluctuation.

The Figure 1.4 (a) shows the rear view of the constant mean velocity lines in the boundary layer of the x = 85.5 cm section. Longitudinal sections are indicated by 5 letters. Of these, E is for the maximum thickness section and A is for the minimum thickness section. The Figure 1.4 (b) shows the mean velocity profiles at the x= 100 cm station in sections A, D and E. The sections in Figure 1.4 (b)are thinner in the A and E sections, and the opposite in the D section, compared to the Blasius profile. As a result of the three-dimensional development of the wave revealed a mechanism. This mechanism is one in which energy is transferred from one opening position to another, and this mechanism has emerged for the disruption of laminar flow.

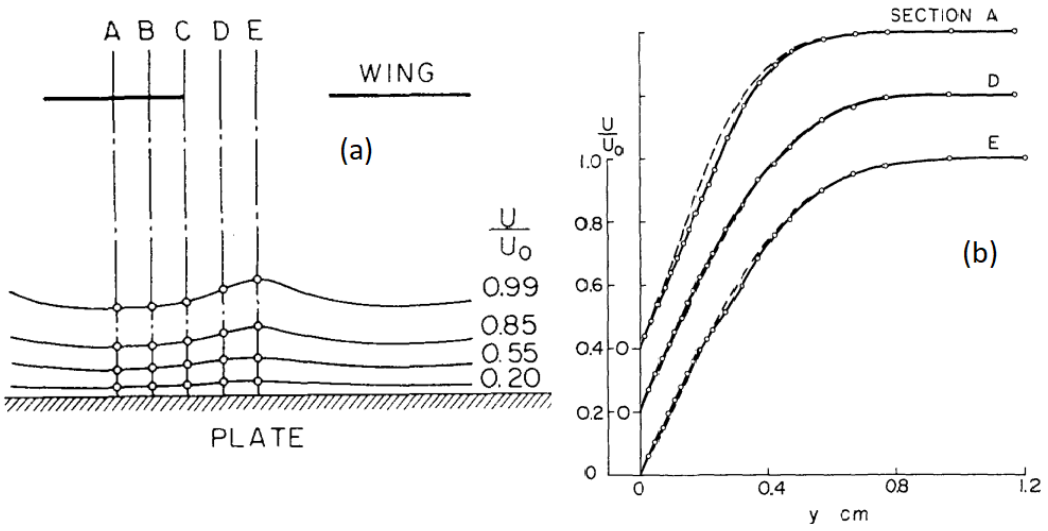

Figure 1.4 : (a) The back view of wings and lines of constant mean velocity in the boundary layer at the station x = 85 cm. (b) The mean velocity profiles at the x=100 cm station in sections A, D and E. The dotted line is the Blasius profile. [3].

One of the transition studies carried out by A. A. Bakchinov et al. in 1995. They carried out transition experiments in a boundary layer with embedded stream-wise vortices [4]. Three-dimensional (3D) perturbations lead to longitudinal vortex structures in flat plate boundary layers, providing conditions for time-dependent instability and changing the nature of the flow. The presence of Tollmien-Schlichting (TS) waves is strongly supported for the transition to turbulence in such flows. In these cases, the transition begins with the appearance of small amplitude traveling time-dependent waves that travel along steady vortices. Gortler and cross flows transition process is similar to that in this case. Gortler vortices and cross-flow vortices are a series of regular downstream vortices produced by body forces. The aim of this study is to shed light on their role in the transition to turbulence and the characteristics of time-related insensitivity. In this study, experiments were carried out in the MT-324 closed circuit low turbulence wind tunnel of the Institute of Theoretical and Applied Mechanics in Novosibirsk. The stream-wise velocity component was measured with a single hot wire probe and a DISA 55M01 anemometer. The probe was calibrated using a Prandtl tube connected to a micromanometer in free flow. Experiments were performed by setting the plate for a zero pressure gradient downstream. Vortices were generated along the aperture direction using a series of roughness elements within the boundary layer. Firstly, the

flow was investigated in the absence of roughness elements while the free flow velocity was set to 8.2 m/s.

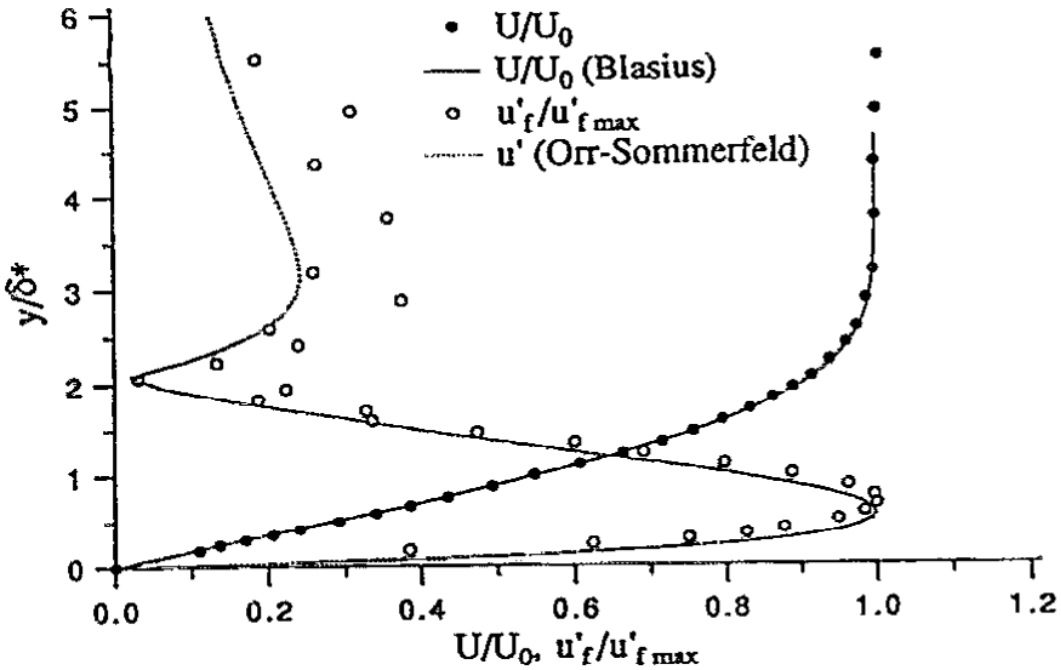

Figure 1.5 : Undisturbed 2-D boundary layer at R=550. (O), mean velocity profile; TS-wave amplitude profile in solid round for F=95; x=550 mm, U_0=8.2 m/s, f=68 Hz [4].

Figure 1.5 shows the boundary layer profile, U(y), at R=550, together with Blasius profile. The displacement thickness (δ^*) was found to be 1.7 mm by evaluating the profile. Also, Figure 1.5 shows the amplitude profile (u'_f) of a TS wave. This wave is excited by the ribbon at a frequency of F=100. TS waves are very tender to pressure gradients. As such, amplification curves are used to give a good representation of the pressure distribution on the plate.

The spectra in Figure 1.6 show the downstream evolution of natural background distortions. In Figure 1.6 (a), a wide wave packet is seen at frequencies between 100 and 200 Hz, while in (b) it is seen that waves grow at frequencies between 150 and 300 Hz. In both cases, a downward shift towards lower frequencies can be observed. Figure 1.6(b) clearly shows the amplification of the second harmonic (400-450 Hz). Below x=500 mm, the spectrum expands and reflects a fully turbulent signal at x= 735 mm. Experiments show that boundary layers modulated in the propagation direction can be unstable relative to TS-type waves. In conclusion, this study provides some

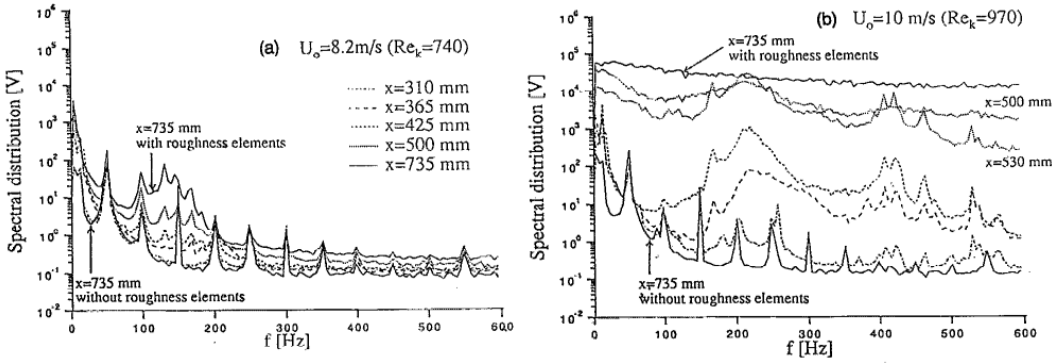

Figure 1.6 : Hot wire spectra at different downstream positions. (a) U_0=8.2 m/s (Re_k=740); (b) U_0=10 m/s (Re_k=970); (.-.), x=310 mm; (—), x=365 mm; (—),x=425 mm; (...), x=500 mm, (-), x=735 mm [4].

evidence that TS waves may be faster due to stream-wise vortices. If the fundamental flow modulation is strong, the dominant instability requires waves with much higher frequencies, and the wave growth and wave amplitude are independent of each other. Thanks to these two studies, it has been understood how the transition conditions should be examined and what should be paid attention to when conducting transition experiments.

Vortex generators have many uses and many experimental and numerical studies have been carried out using them. For instance, HoJoon Shim et al. conducted experimental and numerical studies in 2015 to determine the wake characteristics downstream of a two vane-type vortex generator on a flat plate where the boundary layer is laminar [13]. Much of the previous work has focused on issues such as vortical structure, separation delay and friction reduction by a single vortex generator, so ultimately the purpose of these studies is the efficiency of aerodynamic control. There are few studies in the literature on the wake characteristics of interaction, development and degradation of different downstream vortices. Therefore, in this study, wake characteristics were investigated by conducting experiments in the subsonic wind tunnel of the Korea Aerospace Research Institute (KARI). The experiments were carried out at 10 m/s wind speed. Experimental work was carried out using stereoscopic particle image velocity measurement and in numerical study was carried out to describe in detail the flow field interacting with the vortex generator. In addition, CFD simulations were also performed to better understand the flow physics relationship of multiple vortices inside

the laminar boundary layer. In the experiments, two different lengths of rectangular and triangular generators were tested at three different angles of attack. As a result, wake characteristics were obtained for each states from the PIV data. These states are the overall vortex structure, eddy distribution and downstream distance, as well as the location of the vortex center. When the vortices of the two different vortex generators in this study were compared, it was observed that the triangular one occurred in a lower position. In addition, a general trend cannot be deduced as the geometry and angle of attack greatly alter the wake characteristics.

N. K. Singh conducted a numerical study similar to that of HoJoon Shim et al. in 2018, and this study is a numerical simulation study of the flow behind vortex generators. In this study, vortex generators with rectangular vane on a flat plate were used [5]. Numerically, the time dependent flow behind these vortex generators has been simulated by the immersed boundary (IB) method. In this study, direct forced, one of the IB methods, was preferred due to its high efficiency and simplicity. Two different height vortex generators have been numerically investigated and it has been determined that one of them has conventional and the other low-profile vortex generator features due to their heights. The counter-rotating eddies produced by these generators are characterized and it is investigated how the maximum values of some non-dimensioned properties change in the flow direction. These are streamwise velocity, wall normal velocity, vorticity and vortex force.

Figure 1.7(a) and (b) compare the Blasius profiles obtained in the two cases, respectively, with the velocity component in the mean flow direction. The reason for choosing these figures is to show how the magnitude of the variables changes when different horizontal axis positions are changed. At all streamwise positions in Figure 1.7, the VG-2 case has a more complete streamwise velocity component closer to the wall, from which it is concluded that VG-1 transfers more momentum to the wall than VG-2. In addition, the VG-2 is 2 times the height of the VG-1. As a result, you can see in simulations that passive vortex generators in the laminar boundary layer can simulate flow effectively. If the vortex generator height (0.33 δ) is small, it is shown in the simulations that they do not cause flow separation. It is seen that the vortices in

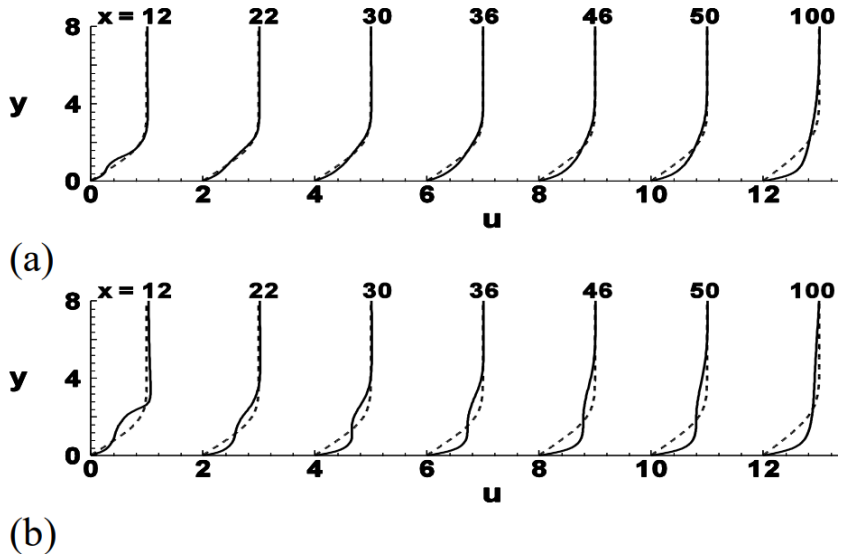

Figure 1.7 : Comprasion of mean streamwise velocity with Blasius profiles (dashed lines) for (a) case VG-1 and (b) VG-2 [5].

the streamwise direction are in the normal direction of the wall and do not show any significant deviation.

A. Urkiola et al. conducted a study similar to the two studies described above in 2017. In this study, a passive vortex generator of rectangular vane mounted on a flat plate was used [14]. They performed computational characterization of the vortex produced by this generator for different vane angles. These generated vortices created are simulated using a negligible pressure gradient. CFD techniques were used to obtain some basic properties of the created vortex. In this study, since the simulations are similar to the conventional vortex generator height sample, there may not be vertical deviation in the center of the vortex along the axial planes according to the simulation results. Consequently, there are two parameters that define the major vortex: the peak vortex at any position streamwise and the half-life radius. As a result, this study developed an estimation model depends on two basic parameters. These parameters are the vane incident angle β and the dimensionless downstream position. The purpose of this model is to simply explain the change in size of the main vortex below the wing, and it has done so for all four different angles of incidence. This model can assist in the design of real VG applications where time and cost can be significantly reduced.

One of the studies for different uses of vortex generators was done by Tian Li et al. in 2023 and this study carried out a numerical investigation of reducing the aerodynamic

drag of a high-speed train using a vortex generator [15]. In this article, only the ICE2 train, which has a simple head car shape and short aerodynamic nose, is examined. The change in the aerodynamic resistance of the train was determined by placing the vortex generators in many determined positions. There are three most important installation locations where the VG is placed. These are the flow separation point, streamline transition position, and the boundary layer mutation. Research shows that the best drag reduction effect is achieved when using VG in the boundary layer of the tail car. The tail car aerodynamic drag and lift reduction is relative to the balance between the separation vortex and the longitudinal vortex, and the vortex generator disrupts this balance, effectively decreasing the strength of the longitudinal vortex, thereby providing a drag reduction. Considering the experimental and numerical studies above, the effects of the vortex generators to be placed in the boundary layer were explained in detail.

Many studies have been done to prevent flow separation in the boundary layer or to delay the transition to turbulence, one of the most notable studies was by J. C. Lin in 1999. This article provides a summary of the development in flow separation control of vortex generators used in turbulent boundary layers [6]. Areas investigated in this study include flow field studies, micro vortex generator progress, and applications to improve high lift performance. The experimental work performed covers topics such as basic flow separation control research, high lift surveys at high Reynolds numbers, and high lift flow field measurement. As a result, it was concluded that vortices produced by vortex generators provide the most effective way to reduce flow separation in turbulent boundary layers. The shape and height of the vortex generators are the most important criteria in reducing flow separation in the boundary layer. As the height of the VG increases, it also increases the friction on the surface, causing a negative effect by increasing exponentially. The performance of Wheeler's wishbone or doublet VGs is less than that of sub-δ-scale wing type VGs. For example, when the ratio h/δ was in the 0.2 to 0.4 range, wing-type VGs were more effective in separation control than wishbone VGs of equivalent height, and were also subject to less device friction. Figure 1.8 shows a comparison of the boundary layer velocity profile near the leading edge of the ramp with the position of the VG elevations. Even when the VG is 0.26

height, the local velocity is 75% above the flow value. The following conclusion is drawn from this; Increasing the height of the VG gives a good increase in local velocity, but negatively increases the drag of the device significantly.

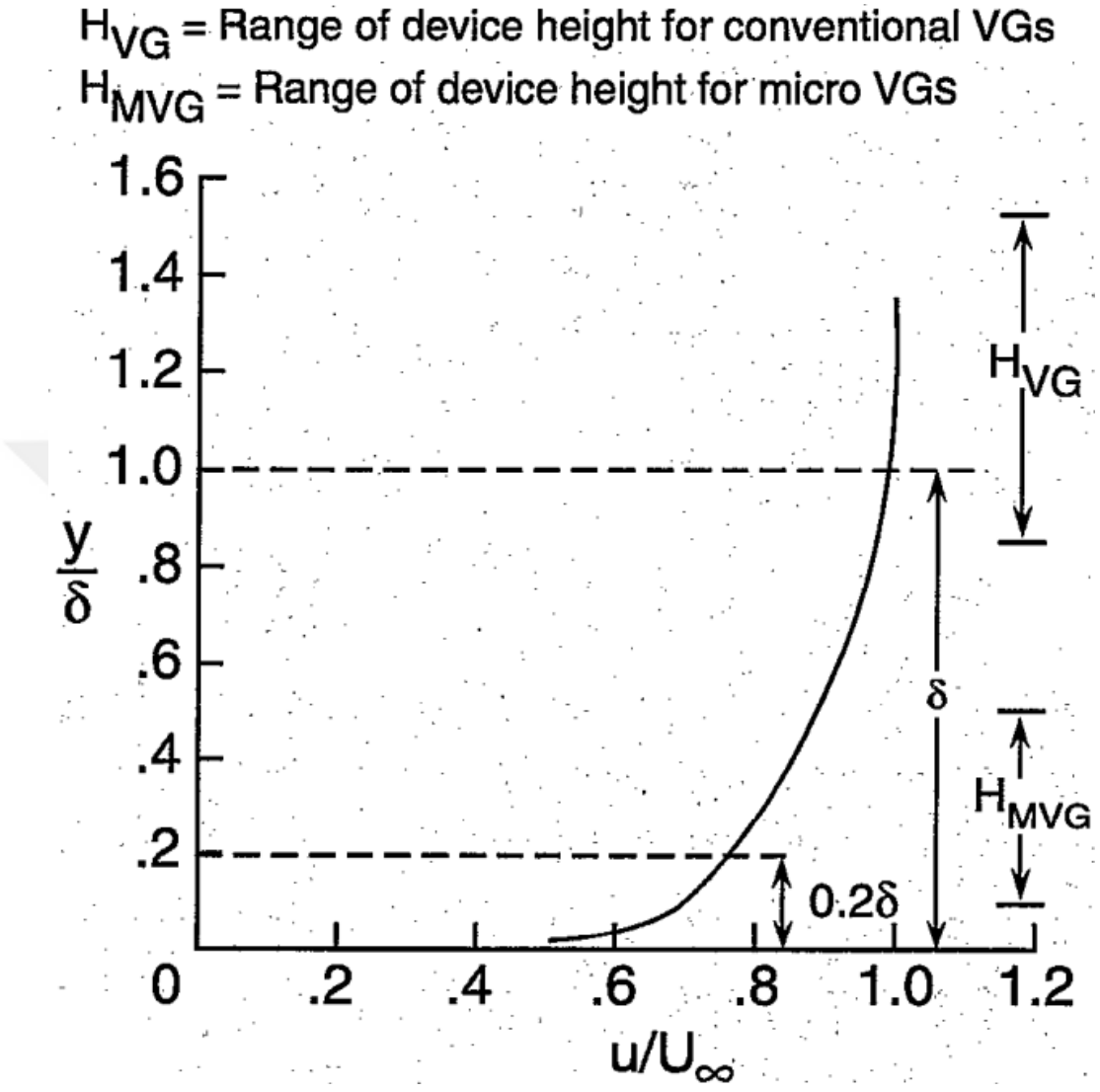

Figure 1.8 : VG height relative to the turbulent boundary layer velocity profile [6].

Using MVGs on high lift airfoils has been found to provide notable performance advancements in lift and drag at near-flight Reynolds numbers. There are many practical advantages to using micro VGs for flow separation control in high lift profiles. These advantages are simple and easy to maintain and also have low device friction and finally very efficient in controlling flow separation in the turbulent boundary layer. Finally, both counter-rotating and co-rotating streamwise vortices were efficient in

reducing flow separation on the wing, but counter-rotating vortices were more efficient than co-rotating eddies for the high lift configuration under consideration.

In another study, S. Shahinfar et al. conducted the possibility of delaying the transition to turbulence in boundary layer flow and the ability of boundary layer lines to scale downstream and reduce skin-friction drag has investigated [7]. In this study, comprehensive studies that tried stabilization of TS waves in 15 different and new MVG configurations using passive flow control strategy are presented and in addition, the stabilizing effect on the TS waves was measured. The experiments were carried out on a 4.2 m long flat plate in a minimum turbulence level (MTL) wind tunnel at the Royal Institute of Technology (KTH) in Stockholm, Sweden. A constant temperature hot wire anemometer was used to measure the velocity signal. Initially, it was started with flat plate experiments at a free-stream velocity of 6 m/s without MVGs at different locations. Figure 1.9 shows the comparison of the mean streamwise velocity profiles at four different flow direction locations of x=(25,50,100,200) cm with Blaius profile.

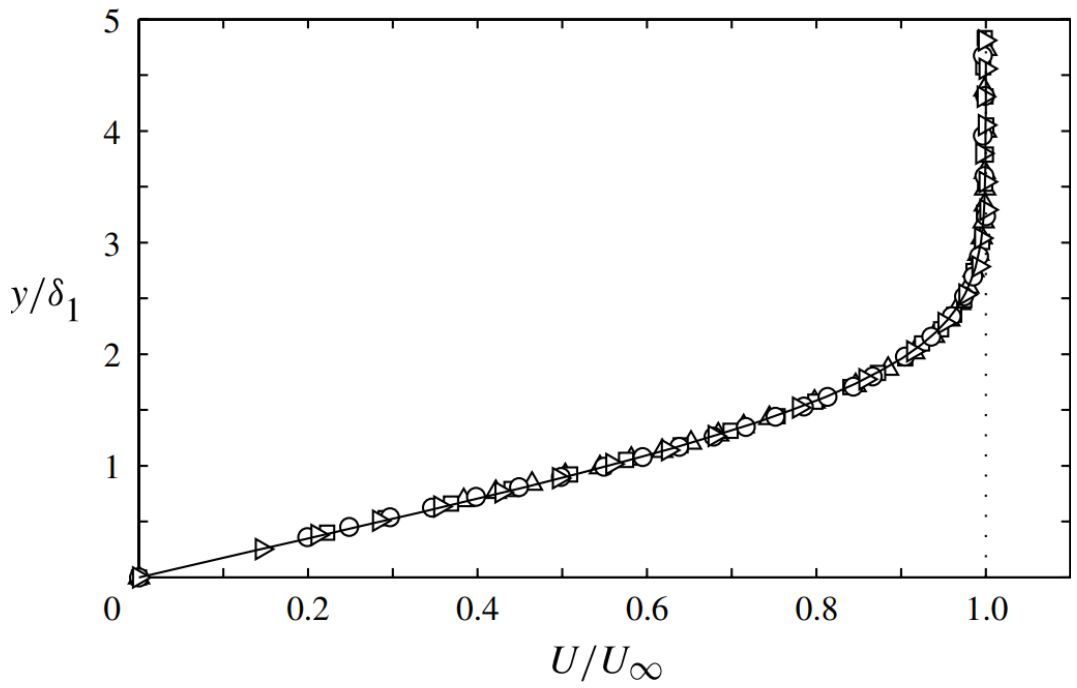

Figure 1.9 : Streamwise velocity profiles measured at different downstream locations. The solidline corresponds to the Blasius solution [7].

Consequently, in this study, streaky base flow from miniature vortex generators is passively produced to delay the transition caused by 2D waves. It has been determined

from the data that the optimal line amplitude is about 30 percent of the free flow velocity, and the purpose of its is to reduce the growth of TS waves. From a comparison of the results of the energy spectra it became clear that the high initial amplitude forcing decreases rapidly and harmonics can never arise when MVGs are used. Finally, it has been shown that the transition initiation can be completely blocked across the measured region by means of an MVG array.

Moreover, L. Siconolfi et al. conducted a different study on flat plate boundary layers using miniature vortex generators (MVGs) at 2015 [16]. This article focuses on simulating and investigating the stability properties of flat plate boundary layers by placing MVGs in an array in the plate propagation direction. In this study, DNSs are implemented to have a detailed description of the velocity domain passing MVGs. The purpose of MVGs is to prevent uncontrolled state and stabilize TS waves by creating constant and stable velocity modulations that reduce growth rates compared to a Blasius BL. Finally, a secondary aim of this article is to validate two non-original global stability analysis-based methodology in cases where passive BL control is performed by MVGs. Thanks to these generators, this article presents stability curves for the boundary layer (BL) for the first time. The behavior of Tollmien-Schlichting (TS) waves is affected by the behavior of the identified unstable modes and local stability analysis results. Therefore, the design of new BL modulators that improve the performance of emerging MVGs is an important information that can shape the future.

One of the studies conducted in 2015 was by Jens H. M. Fransson, and this study investigated the turbulence transition delay using a passive flow control strategy [17]. In addition, in this article, the meaning of reducing skin friction drag has been taken into account. The experiments in this article were obtained using a minimum turbulence level (MTL) wind tunnel at KTH – Stockholm Royal Institute of Technology, Department of Mechanics. MVGs are one of the physical boundary layer modulators, and these modulators show that there are devices that can cause transition delay, and these devices provide transition delay through passive flow control. By using MVGs, different distortions such as single and double oblique waves other than planar Tollmien-Schlichting waves are successfully reduced, thereby providing

transition delay. By using a second array of miniature vortex generators downstream, there is the possibility of delaying the cascade transition to turbulence with passive flow control, while reducing skin friction resistance by at least 65%.

Pedro Paredes et al. in 2018 examined the potential of viable, stationary lines subject to non-modal growth to stabilize a hyper-sonic boundary layer flow using vortex generators and then delay the onset of a boundary layer transition through numerical computations [18]. As a result, in this study, a VG configuration with a single VG array and two separate series with opposite directions was designed on the basis of optimum growth theory. The purpose for which the other was designed to ensure progressive flow instabilities control as well as to reduce amplification of line instabilities from controllers. A single VG array resulted in a 17 percent transition delay, and control configurations based on two separate sequences resulted in a 40 percent transition delay. Thanks to these findings, this study proposes a passive flow control strategy using VGs. Transition delay lines are induced using this strategy where Mack mode instabilities dominate in hyper-sonic BLs.

Additional, Eliane Younes have conducted a detailed analytical experimental study of the transition to turbulence by disrupting the flow using a delta blade pair vortex generator in the air flow channel in January 2023 published [19]. Experiments are performed with Reynolds numbers between 400 and 12000 at various axial positions downstream of the vortex generator, and the flow behavior is characterized in each regime via a frequency analysis. In this study, instantaneous velocity measurements were measured using the Laser Doppler anemometry technique, and by means of these measurements, the dissipation rate of the vortex generators, which increased with distance downstream and then decreased exponentially, was estimated under turbulent flow conditions. Also, a relationship was established between the Strouhal number, which characterizes the vortex instability mechanism, and the Reynolds number.

M. Matsubara and P.H. Alfredsson extensively studied the effect of free-stream turbulence on the development of disturbance in laminar boundary layers and their subsequent conversion to turbulence at 2001 [20]. The experiments were made in the MTL wind tunnel at KTH, Stockholm. This article aims to describe boundary layer

flow exposed to free flow turbulence in the 1 to 6 percent range, and does so through hot wire measurements and flow visualization studies. The most important aim of this study is to in terms of quality and quantity describe FST-induced disturbances in a boundary layer. Wave number spectra were calculated in both the flow direction and propagation direction. As a result, flow visualizations show that upstream structures increase in length downstream, and this is also seen from spectra results. It has been determined from the spectral data that the lengths of the structures in the flow direction are proportional to δ^*. Thanks to the above study, it was understood how to make hot wire measurements and what to pay attention to for my own study, and finally, how to examine the hot wire results.

2. EXPERIMENT

In this study, experiments were carried out in a small-scale wind tunnel with adjustable airflow control. In addition, hot wire measurements were also made. Experiments were carried out in the Trisonic Research Laboratory of the Faculty of Aeronautics and Astronautics of Istanbul Technical University.

2.1 Experimental Set-up

The experiments were carried out on a modular air flow bench (AF10) using one of the experimental modules, the boundary layer module (AF14). The air flow bench (Figure 2.1) consists of a small scale wind tunnel with adjustable airflow control and an electric fan [8]. The unit consists of a solid steel frame on which a fan that supplies air to the aerodynamically shaped constraction and a specially designed plenum chamber via a flow control valve are mounted. Toggle clamps are used to hold the test modules and reliable quick-release couplings are used for the pressure measurement connections.

Figure 2.1 : Air Flow Bench AF10 [8].

All experiments were performed using the boundary layer module (AF14), one of eight different experimental modules that demonstrates the basic principles and phenomena of air flow. This module consists of a channel with a flat plate inside. To diversify experiments, removable duct liners can be added to create the pressure gradient downstream. A flattened Pitot tube measures the total pressure at various distances from the plate surface by positioning the Pitot tube using a micrometer, and hence the velocity, is measured. The Pitot tube is connected to a pressure transducer via a flexible tube equipped with a quick-release coupling.

Figure 2.2 : Boundary Layer module AF14 [8].

Model 239 pressure transducer of Setra brand was used. Model 239 covers a variety of pressure ranges with ±0.073 % FS accuracy over the temperature range of -18 to 80 °C. The Model 239 differential pressure transducer with variable capacitance efficient sensor design provides data with a repeatability of 0.02 % FS and voltage output linearity of ±0.10 % FS [21]. In addition, response time of the transducer is lower than 10ms. During data acquisition mean value of 10000 data is used for each measurement point.

2.2 Hot-Wire Anemometer

The thermal anemometer works on the principle of determining the flow rate due to heat transfer, and the condition causing the heat transfer is the flow of liquid in a small electrically heated sensor placed in the flow. This system has two main methods;

- Constant current mode CCA (Constant Current Anemometer) where the probe temperature changes.

- CTA (Constant Temperature Anemometer) method in which the voltage changes and the probe temperature remains constant.

A typical Wheatstone bridge diagram used in the CCA structure is shown in Figure 2.3.

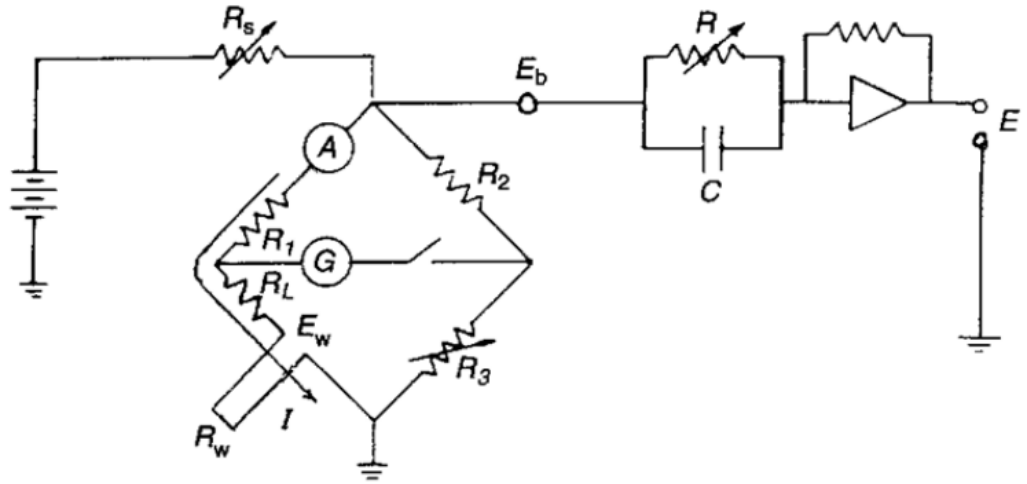

Figure 2.3 : A typical CCA circuit [9].

While hot wire anemometers with constant current circuits were widely used until the development of transistor circuits, the CTA hot wire anemometer started to become widespread from the 1960s on. In this system, the flow of fluid causes heat transfer in the wire, causing the temperature of the wire to drop. As a result, the resistance decreases and the electrical voltage decreases. The voltage is increased so that the wire is kept at the same temperature. Speed measurement is made using these voltage values. Figure 2.4 shows the principle diagram of a typical constant temperature wire anemometer.

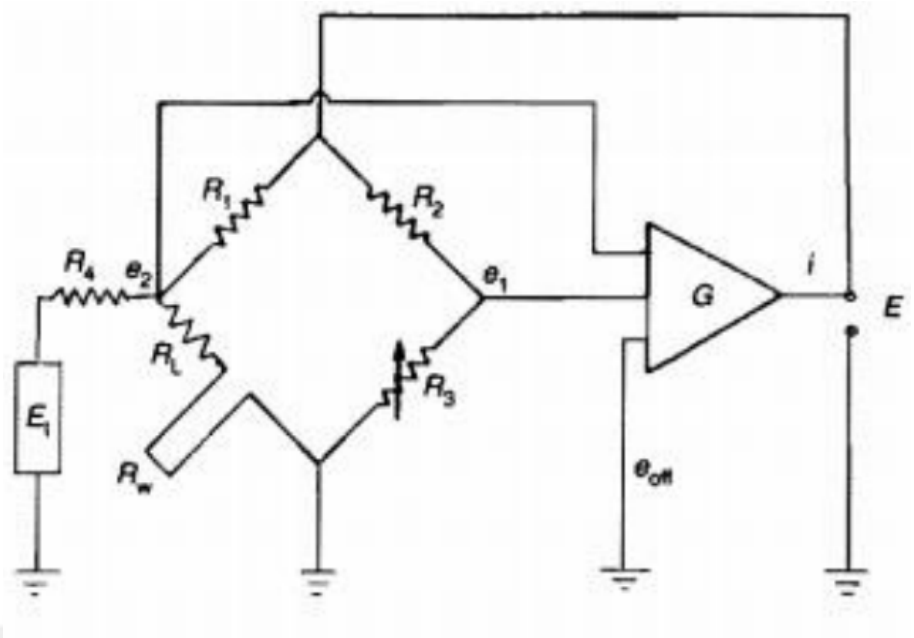

Figure 2.4 : A typical CTA circuit [9].

This circuit is Wheatstone bridge with operational amplifier and adjustable resistor. A current flowing through the wire heats the wire. Convective heat transfer from the sensing wire occurs due to fluid flow and this reduces the temperature, i.e. the resistance of the wire. The purpose here is to keep the temperature of the heated wire and thus its resistance at a constant value. Therefore, besides the cooling effect, the current through the heated wire is increased by using the servo amplifier to ensure that the sensing wire has the initial resistance and temperature [22].

CTA gives the change of velocity at a point with respect to time, and with it density and time dependent statistics can be made. Some examples measured by this are turbulence intensity, autocorrelation, mean velocity, and power spectrum. Dantec StreamLine system was used for data acquisition. Dantec Dynamics offers a complete probe system for use with CTAs and is the most widely used tool today for the measurement and analysis of micro-structures in turbulent gas and liquid flows. The 55P15 boundary layer type probe seen in Figure 2.5 was used in the study. This probe is a constant temperature probe designed for use in boundary layers and is used via a probe support. The probe support is placed on a traverse and moves in line with the given coordinates to determine velocity profiles.

Figure 2.5 : The 55P15 boundary layer type probe.

The probe needs to be calibrated prior to experiments. The aim is to determine the relationship between the CTA output voltage and known flow velocities. The calibration unit is a highly accurate instrument for most hot wire probes used with CTA systems. The hot wire calibrator produces a free jet and the probe is in this jet during calibration. Compressed air is required and speeds between 0.5 m/s and 300 m/s can be adjusted with this system. Figure 2.6 shows the calibration unit. The error between the calibration curve and the data is less than 1 percent for all calibrations.

Figure 2.6 : The Calibration unit.

3. RESULTS AND DISCUSSION

In this study, experiments were carried out in a small-scale wind tunnel with adjustable airflow control. Air under atmospheric conditions was used as the fluid in the experiments. During the experiments, a 27 cm long brass flat plate was used. Spherical balls with a diameter of 1 mm were used as vortex generators. Experiments were carried out for 10 different vortex generator height to boundary layer thickness ratios (h/δ) in the range of 0.4 - 0.8. The variation of the flow in the boundary layer under constant temperature boundary condition is investigated.

Experiments were carried out to determine the positions where the flow in the boundary layer transitions from laminar to turbulent and the effect of the vortex generator on this situation was investigated. In this study, experiments were first performed on the flat plate at different downstream positions flow speeds. Afterwards, a vortex generator was placed on it and the actual experiments were started with different parameters. Free stream velocity and vortex generator position were used as parameters in the experiments. The distance between the VGs was kept constant as 5 mm. In addition, experiments were carried out by adding parts to create a pressure gradient to the experimental setup.

3.1 Base Flow Experiments

In this study, experiments were first performed for the plate at different downstream positions at different flow speeds. These experiments are without vortex generators and without pressure gradient creation. Experiments were taken at different positions for 8,9,10,12 and 15 m/s flow velocity and these experiments results are shown in the tables and figures below.

Table 3.1 : Boundary layer thickness and flow state results of experiments at different positions when the flow velocity is 8 m/s.

X (mm)	V (m/s)	δ	Flow state
50	8,056	1,6	laminar flow
100	8,04	2	laminar flow
120	8	2,1	laminar flow
150	8,059	2,4	laminar flow
200	8,05	2,8	laminar flow
250	8,07	3,3	transition

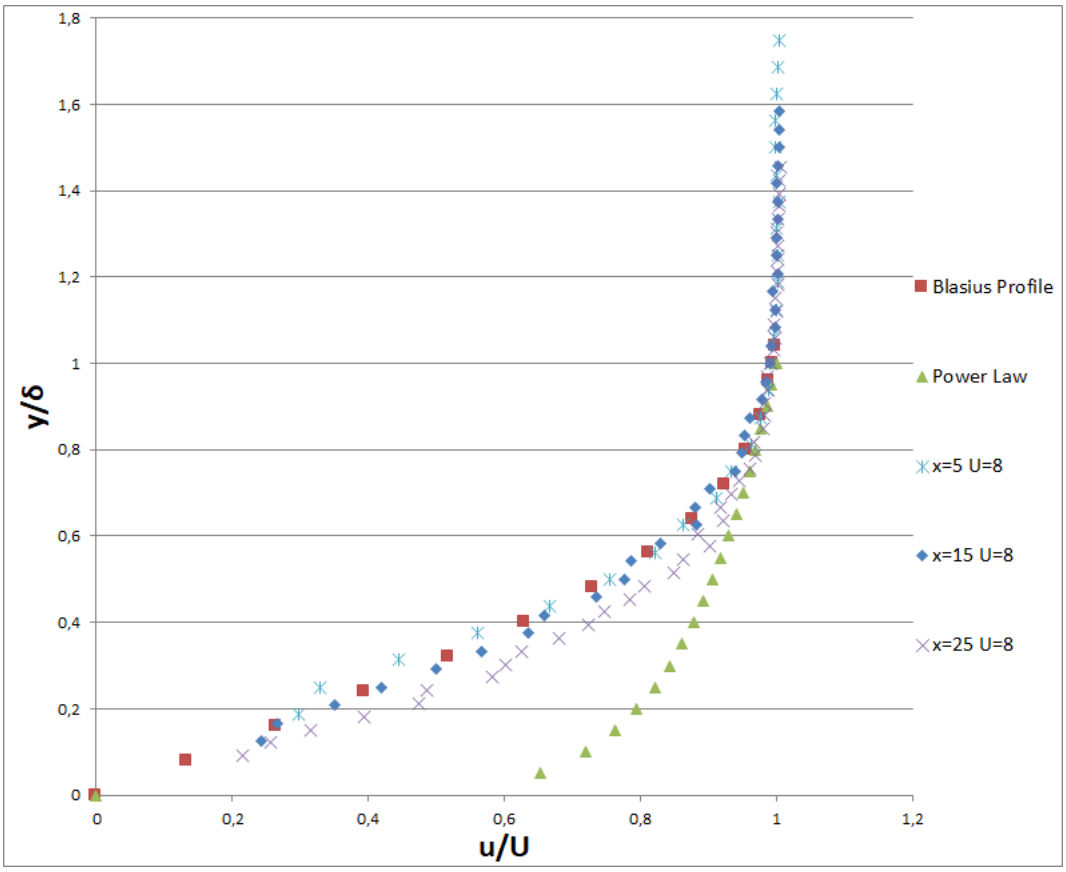

Figure 3.1 : Boundary layer profiles at x=5, x=15 and x=25 cm for 8 m/s flow velocity.

In the Table 3.1, boundary layer thicknesses(δ) and flow states in the experiments at different positions at 8 m/s flow velocity are shown. According to this table, the flow in the boundary layer for 8 m/s flow velocity seems to be laminar everywhere, only at the beginning of the transition zone according to the result of the experiment at 25 cm. Boundary layer velocity profiles are given in Figure 3.1.

Table 3.2 : Boundary layer thickness and flow state results of experiments at different positions when the flow velocity is 9 m/s.

X (mm)	V (m/s)	δ	Flow state
50	8,98	1,4	laminar flow
80	9,038	1,8	laminar flow
90	9,05	1,9	laminar flow
100	9,05	2	laminar flow
120	9,06	2,1	laminar flow
150	9,07	2,5	laminar flow
200	9,088	2,7	laminar flow
250	9,07	3,1	transition

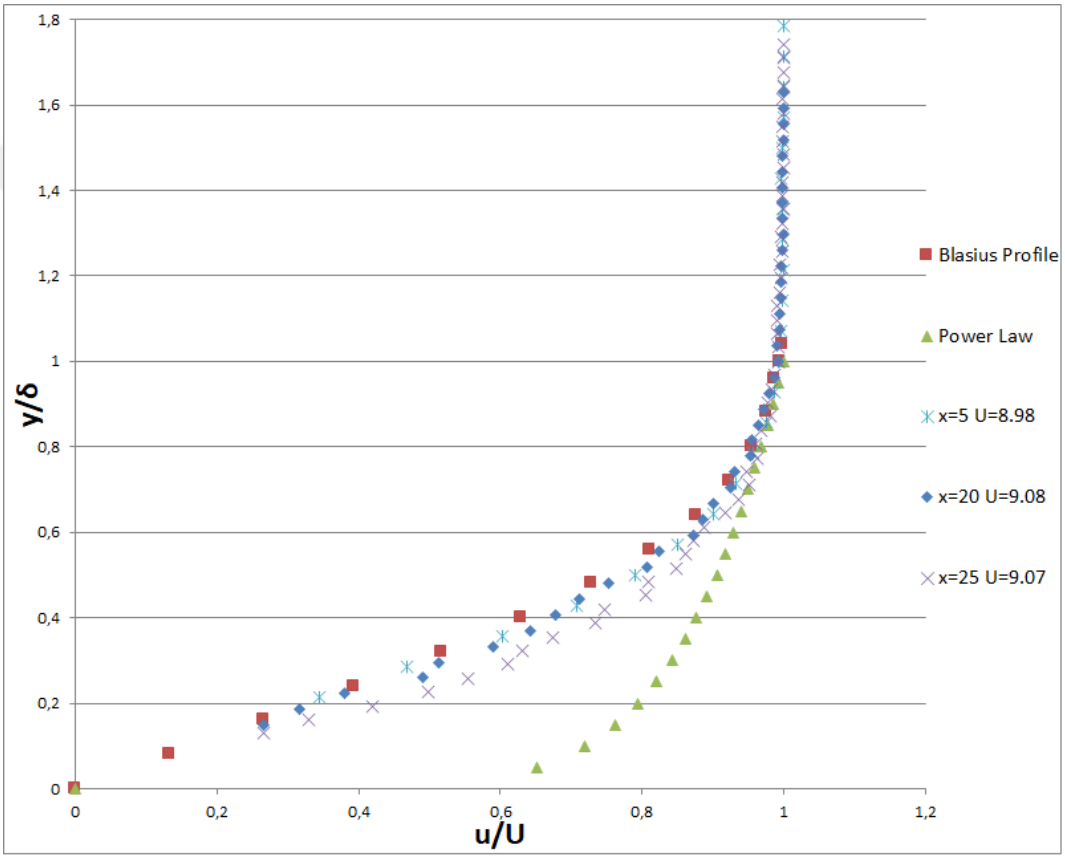

Figure 3.2 : Boundary layer profiles at x=5, x=20 and x=25 cm for 9 m/s flow velocity.

In the table 3.2 above, boundary layer thicknesses and flow states in the experiments at different positions at 9 m/s flow velocity are shown. According to this table, the flow in the boundary layer for 9 m/s flow velocity seems to be laminar everywhere, except for the experiment at 25 cm only. As can be see from the Figure 3.2 boundary layer profiles fits well Blasius laminar solution along the plate except for x=250 mm where transition

phase starts. It has been determined that the results of the experiments performed with 9 m/s flow velocity are very close as the results of the experiments performed with 8 m/s flow velocity, when the flow states are examined in terms of location.

Table 3.3 : Boundary layer thickness and flow state results of experiments at different positions when the flow velocity is 10 m/s.

X (mm)	V (m/s)	δ	Flow state
30	10	1,1	laminar flow
50	10,03	1,4	laminar flow
60	10,03	1,5	laminar flow
70	10,05	1,5	laminar flow
80	10,05	1,7	laminar flow
100	10,07	1,9	laminar flow
120	10	2	laminar flow
150	10,11	2,4	transition
200	10,14	2,7	transition
250	10,11	3,3	transition

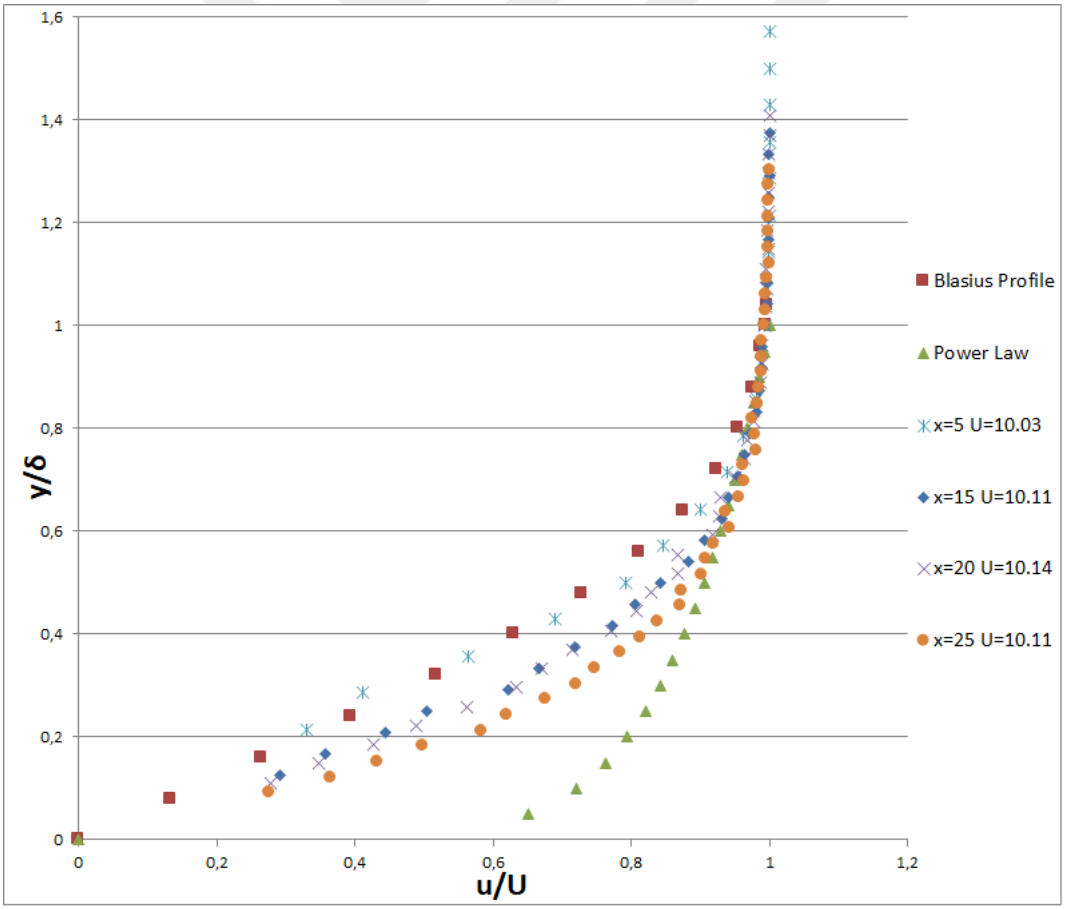

Figure 3.3 : Boundary layer profiles at x=5, x=15, x=20 and x=25 cm for 10 m/s flow velocity.

In the table 3.3 above, boundary layer thicknesses and flow states in the experiments at different positions at 10 m/s flow velocity are shown. According to this table, it is seen in the experiments performed for a flow rate of 10 m/s that the flow in the boundary layer starts to change from laminar to turbulent after 15 cm, that is, according to the test result at 25 cm, the flow in the boundary layer appears in the transition zone. You can see the accuracy of these results in Figure 3.3.

Table 3.4 : Boundary layer thickness and flow state results of experiments at different positions when the flow velocity is 12 m/s.

X (mm)	V (m/s)	δ	Flow state
50	12	1,2	laminar flow
100	12	1,8	laminar flow
120	12	1,9	laminar flow
150	12	2,1	laminar flow
200	12	2,5	transition
250	12	3	transition

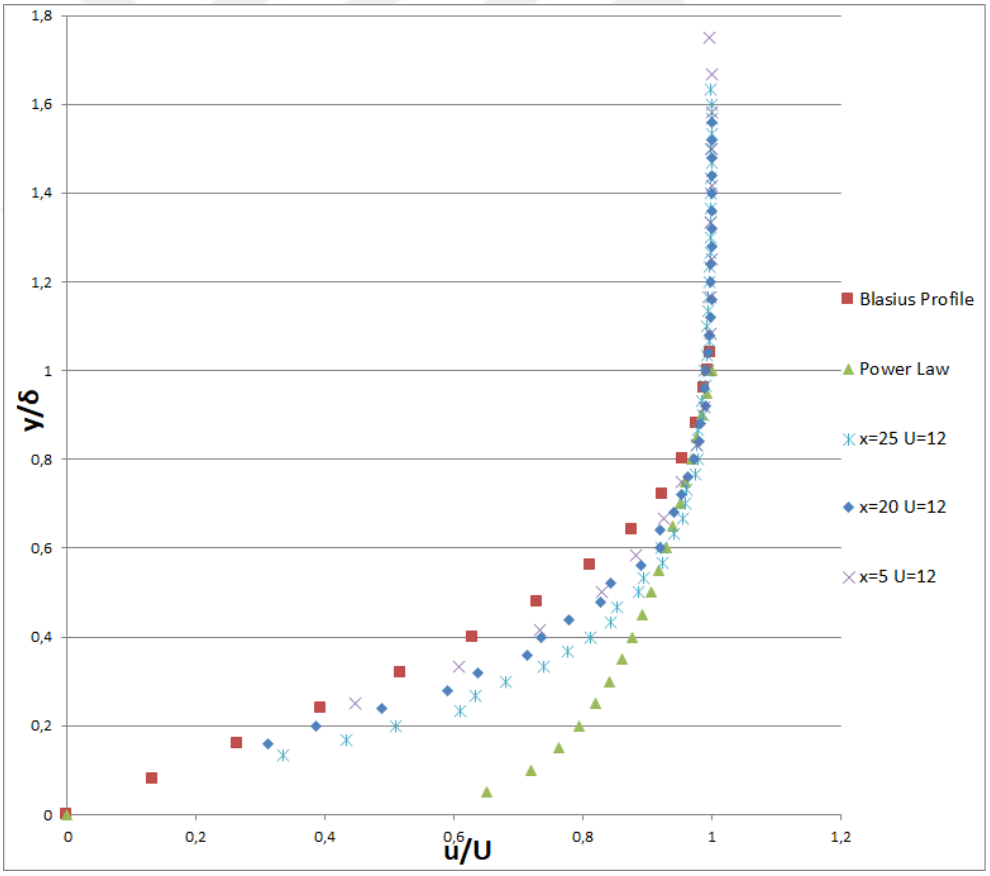

Figure 3.4 : Boundary layer profiles at x=5, x=20 and x=25 cm for 12 m/s flow velocity.

Table 3.5 : Boundary layer thickness and flow state results of experiments at different positions when the flow velocity is 15 m/s.

X (mm)	V (m/s)	δ	Flow state
30	15	0,95	laminar flow
50	15	1,24	laminar flow
100	15	1,6	laminar flow
120	15,05	1,7	transition
150	15	1,8	transition
200	15	2,1	transition
250	15	2,8	turbulent flow

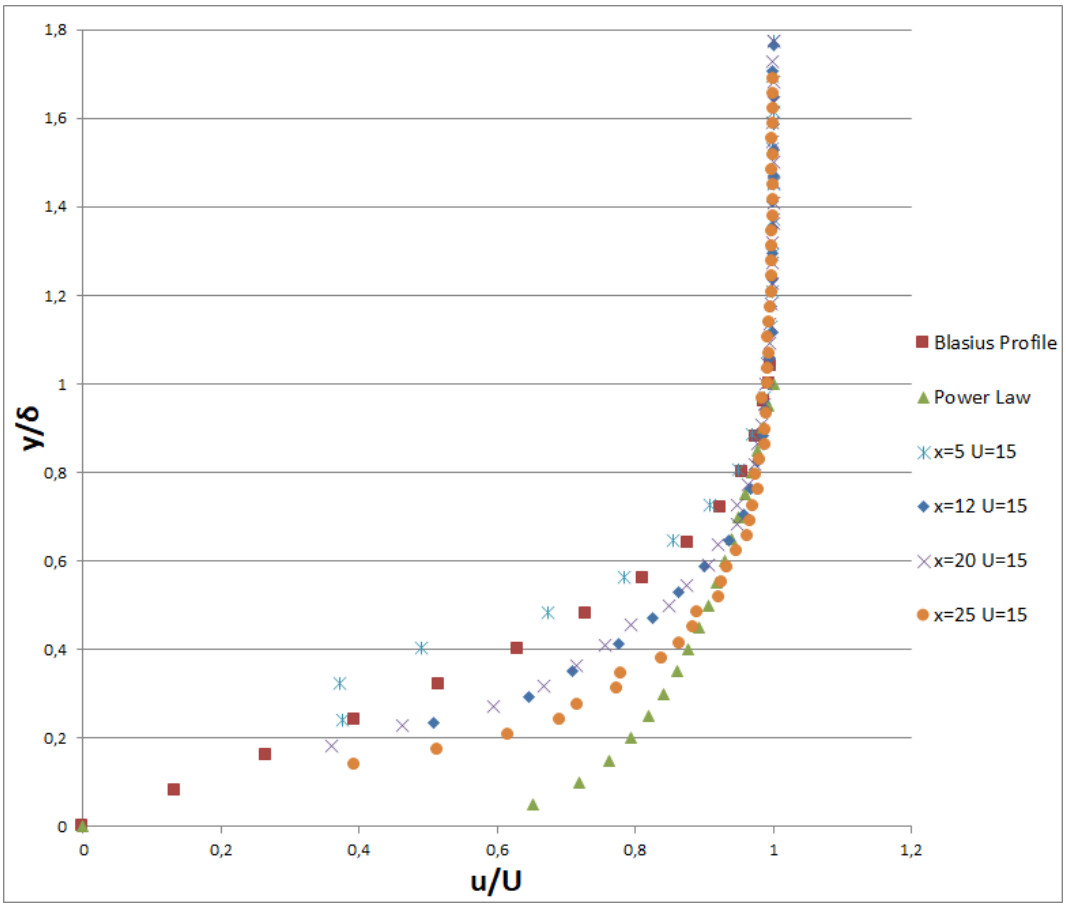

Figure 3.5 : Boundary layer profiles at x=5,x=12, x=20 and x=25 cm for 15 m/s flow velocity.

In the Table 3.4 and Table 3.5, boundary layer thicknesses and flow states in the experiments at different positions at 12 m/s and 15 m/s flow velocity are shown. As can be seen from Figure 3.5, the boundary layer profiles fit well Blasius laminar solution up to x=120 mm in the flat plate. However, when the flat plate reaches 25 cm, it is seen that the flow in the boundary layer starts to change from transition to turbulence.

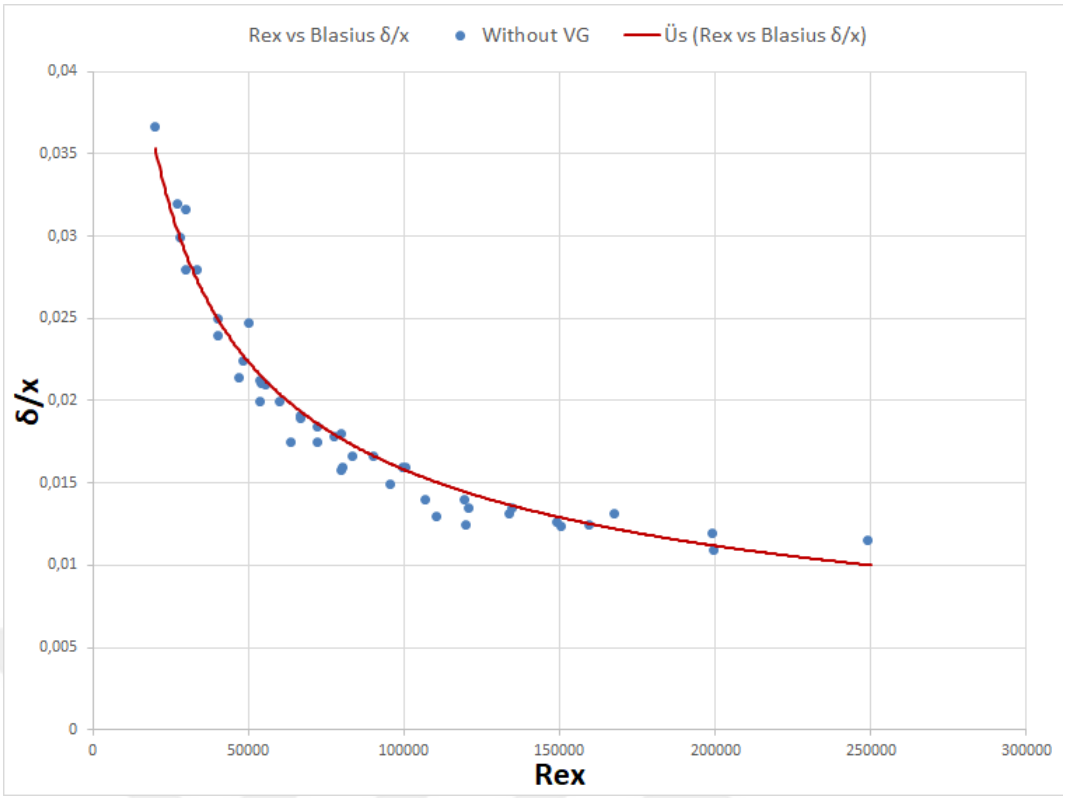

Figure 3.6 : Reynolds number (Re) versus boundary layer thickness to positions ratio (δ/x) from leading edge without a vortex generator

Figure 3.6 shows the graph of boundary layer thickness to position ratio (δ/x) comparison with Reynolds number of experiments without vortex generator at different velocities. The Reynolds number is dependent on flow velocity, density, viscosity, and length, and so experiments measured at the same position and velocity will have the same Reynolds numbers. As seen in the graph, the results of most of the experiments are consistent with the theoretical calculations, that is, around the Blasius curve. Only the point where the Re number is 250000 is far from the curve because this is the experiment at 25 cm on a flat plate with the free stream velocity set to 15 m/s, and according to the result of this experiment, the boundary layer flow is turbulent. It is expected that that point will be far from the curve anyway.

3.2 Vortex Generator Experiments

In this section, the results of the experiments with vortex generators are shown by giving tables and boundary layer profiles. Spherical balls with a diameter of 1 mm were used as vortex generators. Experiments were taken by placing the vortex generators

in two different locations. Since the flat plate is 27 cm long, it was decided that the most suitable places to place the vortex generators are 5 and 12 cm. Experiments were carried out by placing 10 vortex generators at equal intervals at these locations. The distance between the VGs was kept constant as 5 mm.

3.2.1 Experiments with VGs placed at 5 cm

Table 3.6 : Boundary layer thickness and flow state results of experiments at different locations with vortex generators placed at 5 cm when flow velocity is 8 m/s and 9 m/s.

X (mm)	V (m/s)	δ	Flow state
100	8,037	2	laminar flow
250	8,03	3,4	transition
200	8,4	3,5	turbulent flow
80	9,15	1,8	laminar
90	9	1,9	transition
100	9	2	transition
150	9	2,6	transition
200	9	3,7	turbulent flow
250	9	4,3	turbulent flow

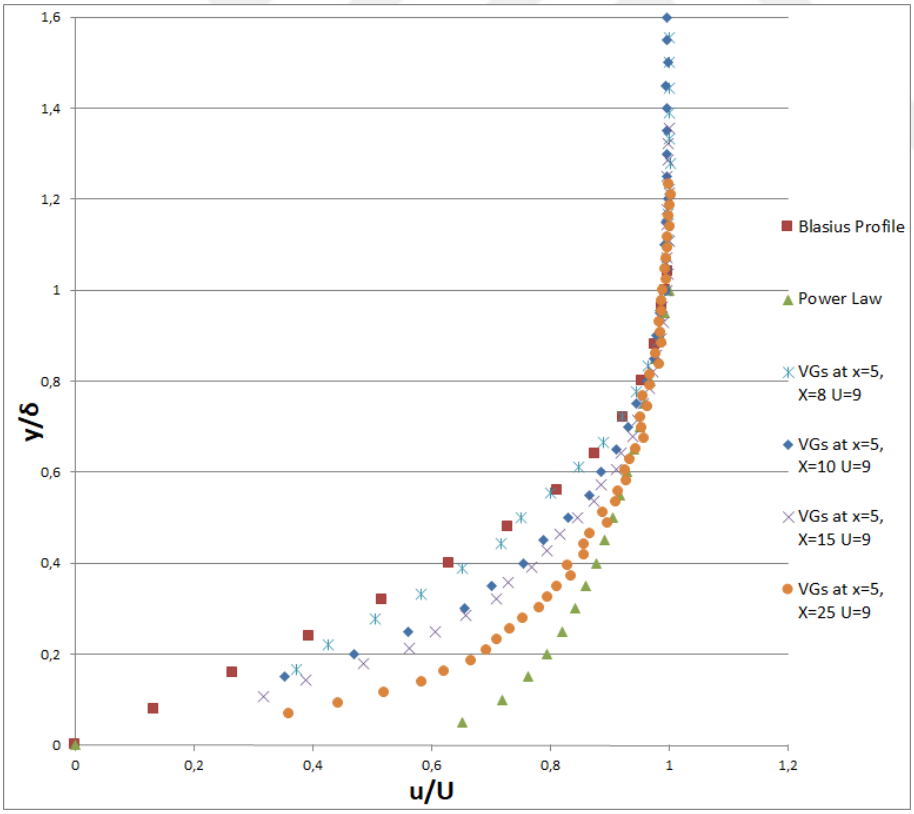

Figure 3.7 : Boundary layer profiles at x=8,x=10, x=15 and x=25 cm with vortex generators at 5 cm for a flow velocity of 9 m/s.

Boundary layer shape and thickness obtained from experiments performed at 8 and 9 m/s velocities when the vortex generators were placed at 5 cm are given in the table above. According to these results, the experiments carried out at 8 m/s velocity, it was found that the flow in the boundary layer is laminar in the part after the vortex generators. It was observed that it was found that flow passing through VGs maintains a certain distance laminarity. Transition starts approximately at X=25cm, 20 cm downstream distance (δx/h=200) from the VGs. In the experiments performed when the velocity is 9 m/s, it is seen that the flow in the boundary layer after the vortex generators remains laminar by 3-4 cm. Then, it was determined that the flow up to 15 cm started to turn into turbulence in the transition zone after that. According to the results of the experiment performed at 20 cm, it was found that the flow in the boundary layer was turbulent. In other words, when looked at as a result, it was determined that the vortex generators could not make the flow turbulent when the velocity was 8 m/s, but made the flow in the boundary layer turbulent when it was 9 m/s.

Table 3.7 : Boundary layer thickness and flow state results of experiments at different locations with vortex generators placed at 5 cm when flow velocity is 10 m/s.

X (mm)	V (m/s)	δ	Flow state
60	10	1,5	laminar flow
70	10	1,6	laminar flow
80	10	1,8	transition
100	10,13	2,2	transition
150	10,1	3,3	turbulent flow
200	10,03	4,1	turbulent flow
250	10	5,2	turbulent flow

In the Table 3.7 above, boundary layer thickness and flow state results of the experiments performed at 10 m/s velocities when the vortex generators were placed at 5 cm are given. According to these results of the experiments carried out at 10 m/s speed, it was determined that the flow in the boundary layer continues laminar for 3 cm in the part after the vortex generators. As a result of the experiment performed at 8 cm, it was determined that the flow in the boundary layer transition from laminar to the transition, and as a result of the experiment at 15 cm, it was observed that the flow became transition to turbulent. Figure 3.8 shows that the flow in the boundary layer is fully turbulent at 25 cm, thanks to the vortex generators.

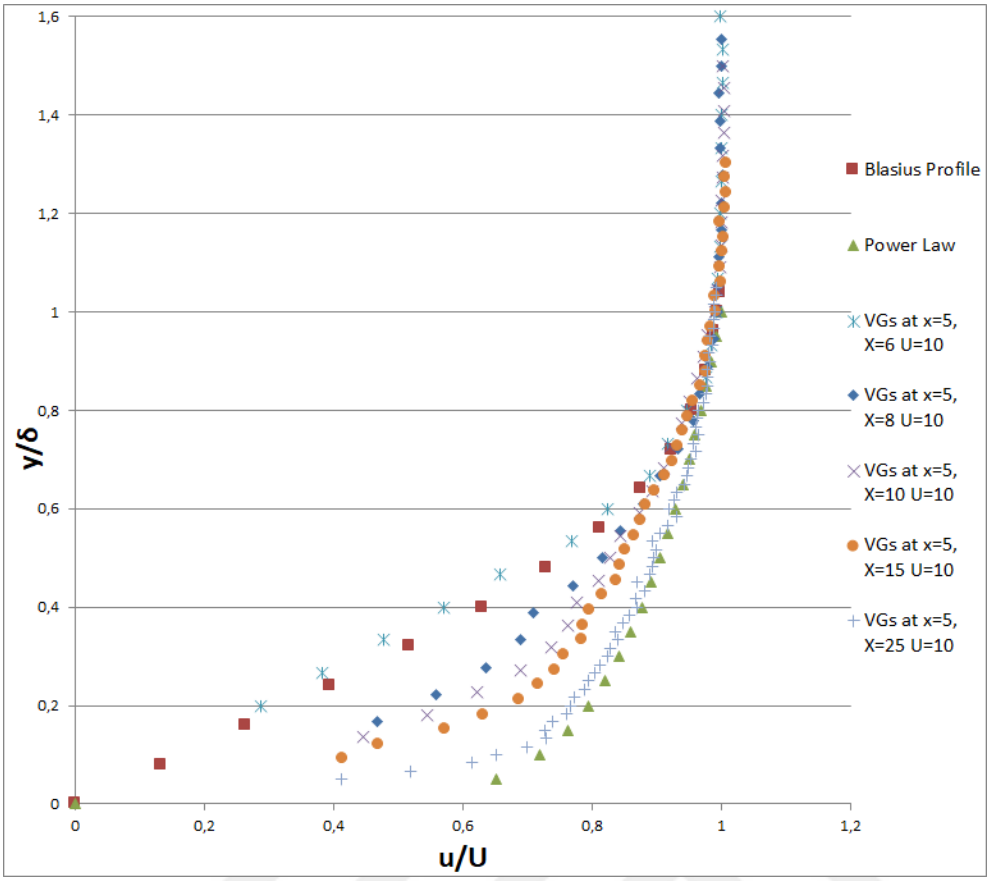

Figure 3.8 : Boundary layer profiles at x=6,x=8,x=10, x=15 and x=25 cm with vortex generators at 5 cm for a flow velocity of 10 m/s.

Table 3.8 : Boundary layer thickness and flow state results of experiments at different locations with vortex generators placed at 5 cm when flow velocity is 12 m/s.

X (mm)	V (m/s)	δ	Flow state
60	12	1,5	laminar flow
80	12	1,8	transition
100	12	2,4	transition
150	12	3,7	turbulent flow
200	12	4,4	turbulent flow
250	12	5,1	turbulent flow

Table 3.9 : Boundary layer thickness and flow state results of experiments at different locations with vortex generators placed at 5 cm when flow velocity is 15 m/s.

X (mm)	V (m/s)	δ	Flow state
60	15	1,3	laminar flow
80	15	2,1	transition
100	14,91	2,5	turbulent flow
150	15	3,5	turbulent flow
200	15	4,4	turbulent flow
250	15	4,9	turbulent flow

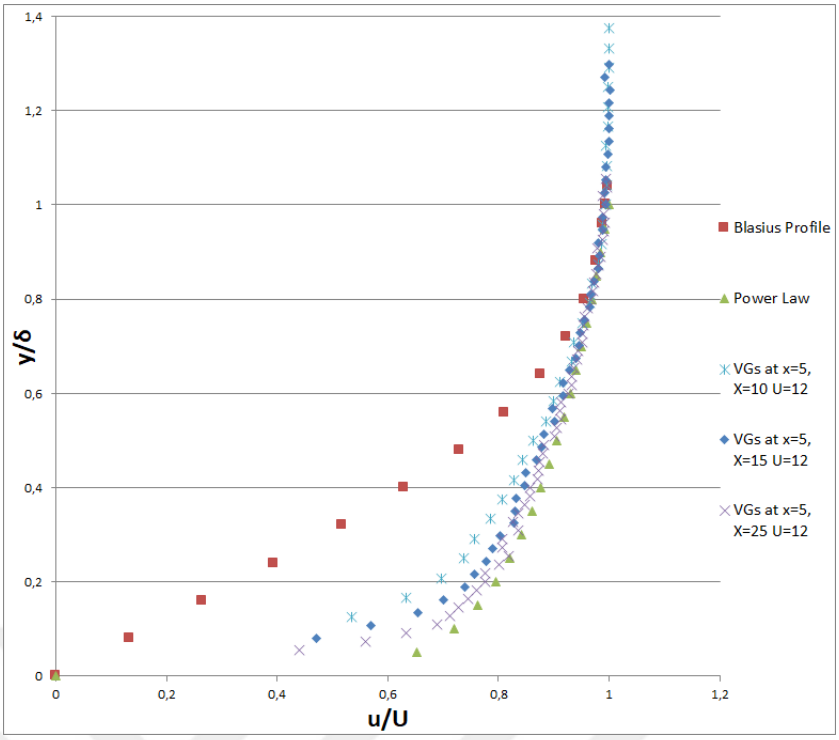

Figure 3.9 : Boundary layer profiles at x=10, x=15 and x=25 cm with vortex generators at 5 cm for a flow velocity of 12 m/s.

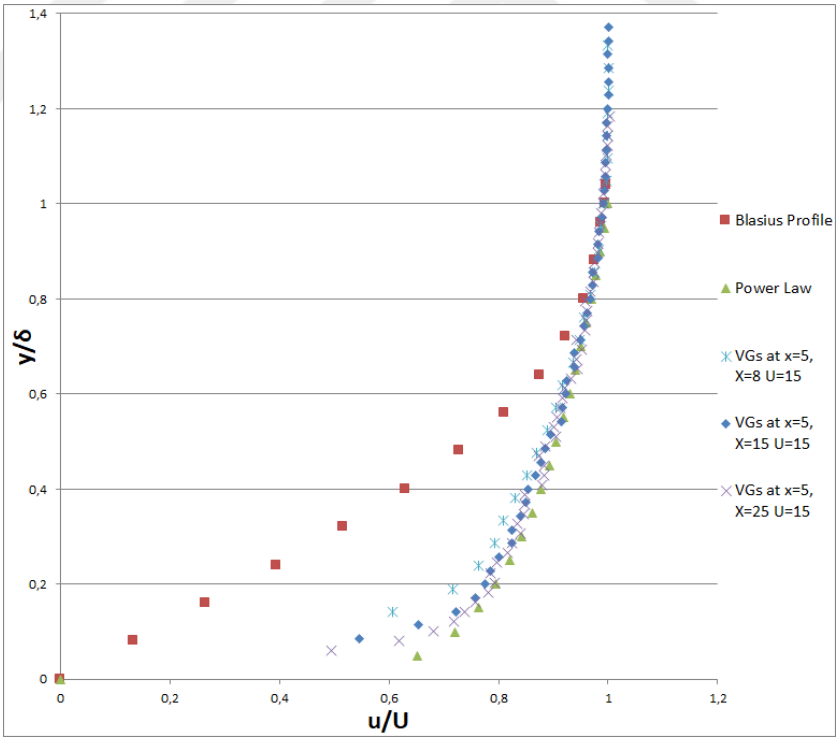

Figure 3.10 : Boundary layer profiles at x=8, x=15 and x=25 cm with vortex generators at 5 cm for a flow velocity of 15 m/s.

3.2.2 Experiments with VGs placed at 12 cm

Table 3.10 : Boundary layer thickness and flow state results of experiments at different locations with vortex generators placed at 12 cm when flow velocity is 8 m/s.

X (mm)	V (m/s)	δ	Flow state
150	8,07	2,4	laminar flow
160	7,97	2,6	laminar flow
170	8	2,8	transition
200	7,93	3,1	transition
250	8	3,3	transition

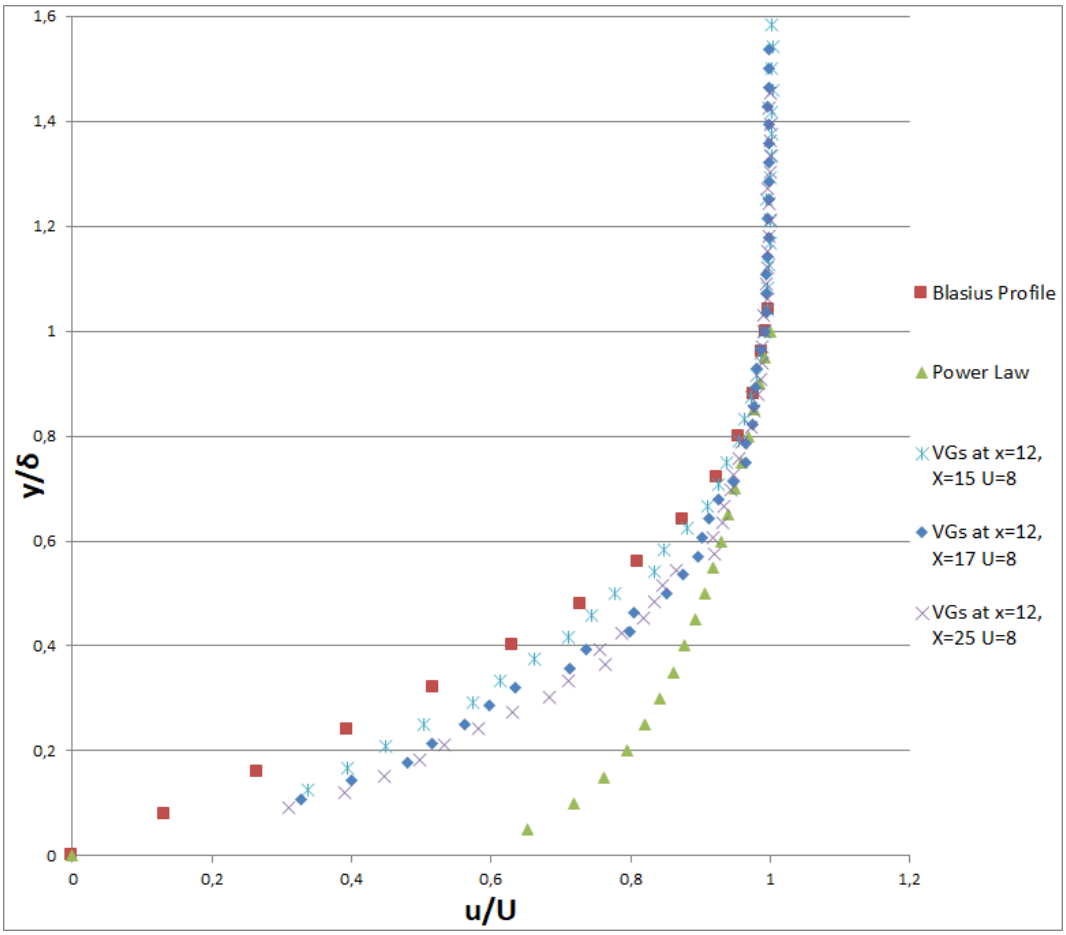

Figure 3.11 : Boundary layer profiles at x=15, x=17 and x=25 cm with vortex generators at 12 cm for a flow velocity of 8 m/s.

In the Table 3.10 and Figure 3.11, the results of the experiments performed with eddy generators placed at 12 cm on a flat plate and the flow velocity set to 8 m/s are given. According to these results, it has been determined that the flow in the boundary layer is in the transition zone and does not go into turbulence.

Table 3.11 : Boundary layer thickness and flow state results of experiments at different locations with vortex generators placed at 12 cm when flow velocity is 9 m/s.

X (mm)	V (m/s)	δ	Flow state
150	9	2,1	transition
160	9	2,3	transition
170	9	2,4	transition
200	9	2,6	transition
250	9	3	transition

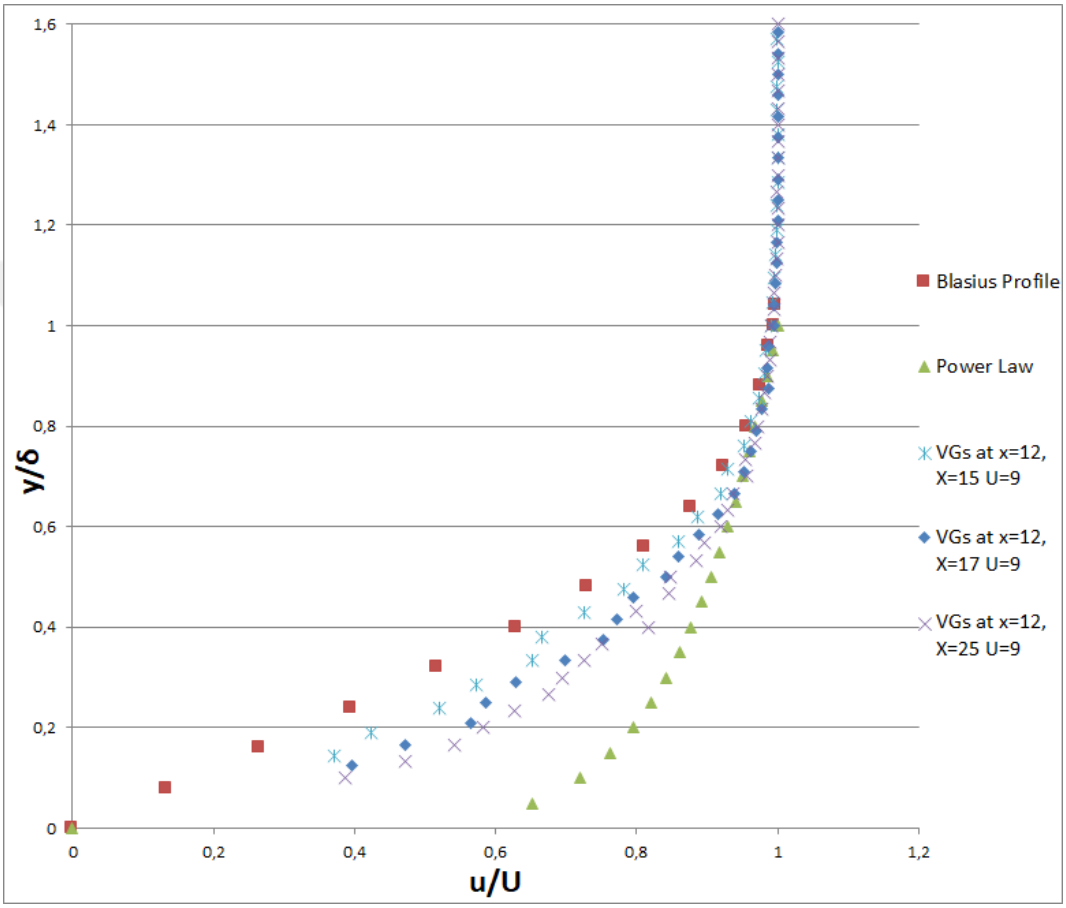

Figure 3.12 : Boundary layer profiles at x=15, x=17 and x=25 cm with vortex generators at 12 cm for a flow velocity of 9 m/s.

According to the results of the experiments performed with vortex generators placed on a flat plate at 12 cm and a flow velocity set to 9 m/s, it was determined that the flow in the boundary layer transitioned from laminar to transition at 15 cm. In other words, it has been determined that the transition starting point is 15 cm. Looking at the test result at 25 cm, it can be seen that the flow in the boundary layer is still in the transition zone and does not pass into turbulence.

Table 3.12 : Boundary layer thickness and flow state results of experiments at different locations with vortex generators placed at 12 cm when flow velocity is 10 m/s.

X (mm)	V (m/s)	δ	Flow state
150	10	2,1	transition
160	10	2,2	transition
170	10	2,3	transition
200	10	2,6	transition
250	10	3,2	transition

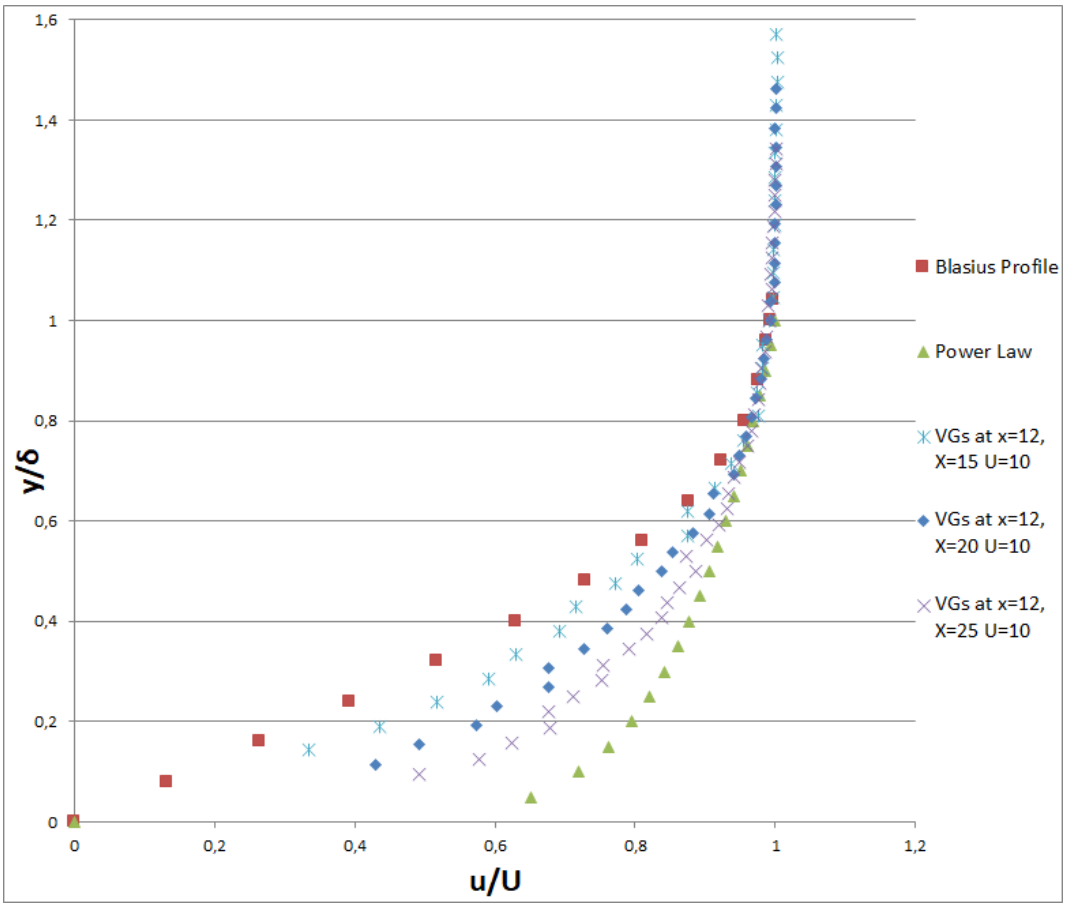

Figure 3.13 : Boundary layer profiles at x=15, x=20 and x=25 cm with vortex generators at 12 cm for a flow velocity of 10 m/s.

According to the results of the experiments performed with vortex generators placed on a flat plate at 12 cm and a flow velocity set to 10 m/s, it was determined that the flow in the boundary layer transitioned from laminar to transition at 15 cm. In other words, it has been determined that the transition starting point is 15 cm. Looking at the test result at 25 cm, it is seen that the flow in the boundary layer is at the end of

the transition zone, that velocity profiles are very close to fully turbulent profiles (1/7th degree power law)

3.3 Experiments With Pressure Gradient

Experiments were carried out by mounting parts to create a positive pressure gradient on the air flow bench. The following tables and figures show the results of the pressure gradient experiments.

Table 3.13 : Boundary layer thickness and flow state results of experiments performed in different locations with positive pressure gradient effect when flow velocity is 8.35 m/s.

X (mm)	V (m/s)	δ	Flow state	$\frac{\partial P}{\partial x}$
100	8,35	2,3	laminar flow	0,166
120	8,37	2,7	laminar flow	0,167
130	8,4	2,8	laminar flow	0,168
140	8,37	2,9	laminar flow	0,167
150	8,38	3,1	laminar flow	0,168
200	8,37	5,1	turbulent flow	0,167

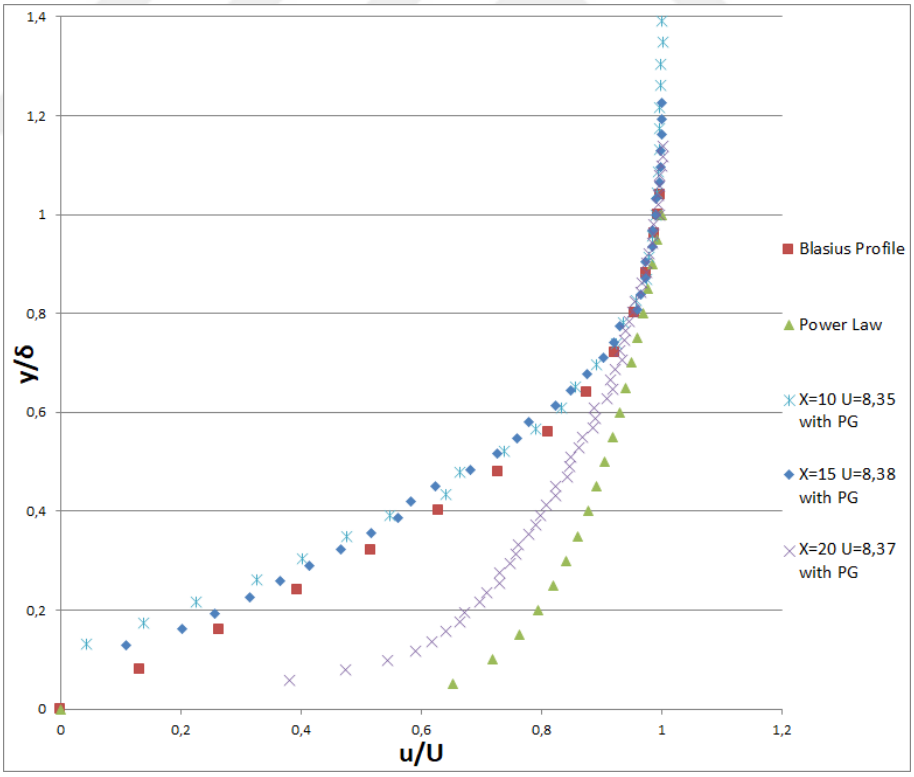

Figure 3.14 : Boundary layer profiles at x=10, x=15 and x=20 cm with pressure gradient for a flow velocity of 8,35 m/s.

Since the parts forming the pressure gradient narrow the area where the flow comes from on the air flow bench, the flow velocity can be adjusted to the lowest 8.3-8.4 range. Therefore, experiments were carried out at these speeds first. Table 3.13 and Figure 3.14 above show the results of the first experiments with pressure gradient. According to the results, it is seen that the flow in the boundary layer is laminar in many locations, but when it comes to 20 cm, it is determined that the flow in the boundary layer turns into turbulence.

Table 3.14 : Boundary layer thickness and flow state results of experiments performed in different locations with positive pressure gradient effect when flow velocity is 9 m/s.

X (mm)	V (m/s)	δ	Flow state	$\frac{\partial P}{\partial x}$
90	9	2,3	laminar flow	0,193
100	9	2,4	laminar flow	0,193
120	9	2,5	laminar flow	0,194
150	8,96	3,1	laminar flow	0,192
200	9	4,7	turbulent flow	0,193

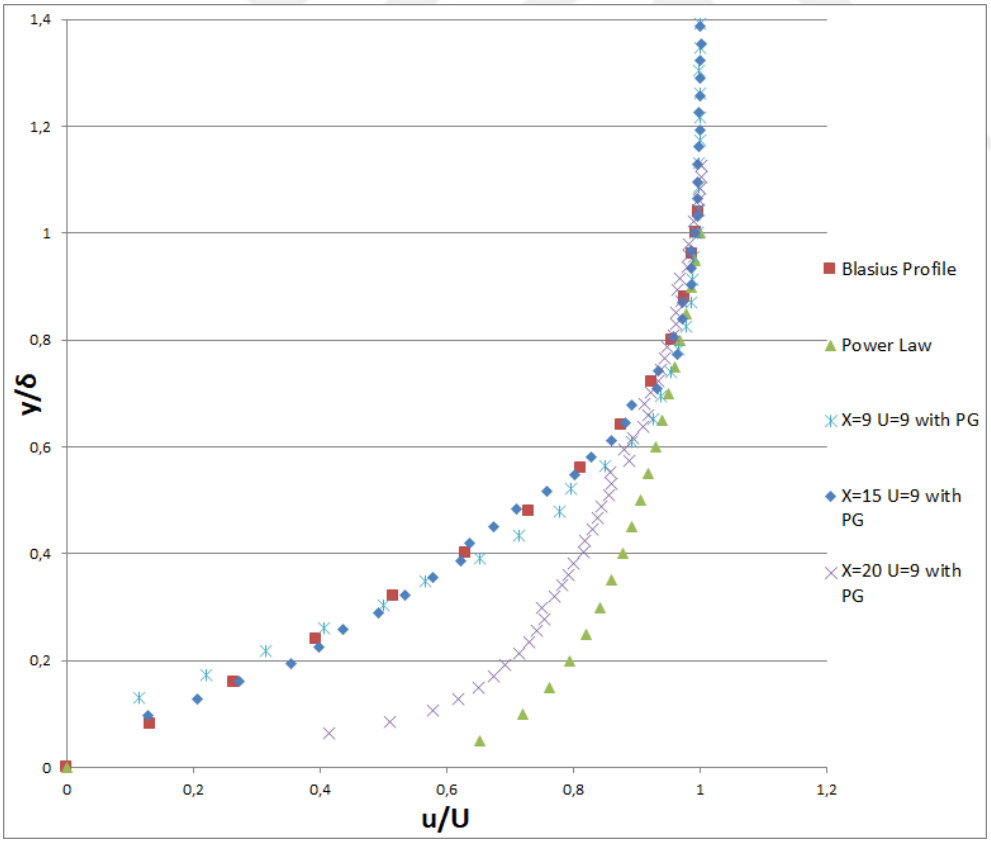

Figure 3.15 : Boundary layer profiles at x=9, x=15 and x=20 cm with pressure gradient for a flow velocity of 9 m/s.

Table 3.15 : Boundary layer thickness and flow state results of experiments performed in different locations with positive pressure gradient effect when flow velocity is 10 m/s.

X (mm)	V (m/s)	δ	Flow state	$\frac{\partial P}{\partial x}$
70	10	1,7	laminar flow	0,239
80	10	1,8	laminar flow	0,238
100	10	2	laminar flow	0,239
150	10	2,7	transition	0,240
200	10	4,9	turbulent flow	0,239

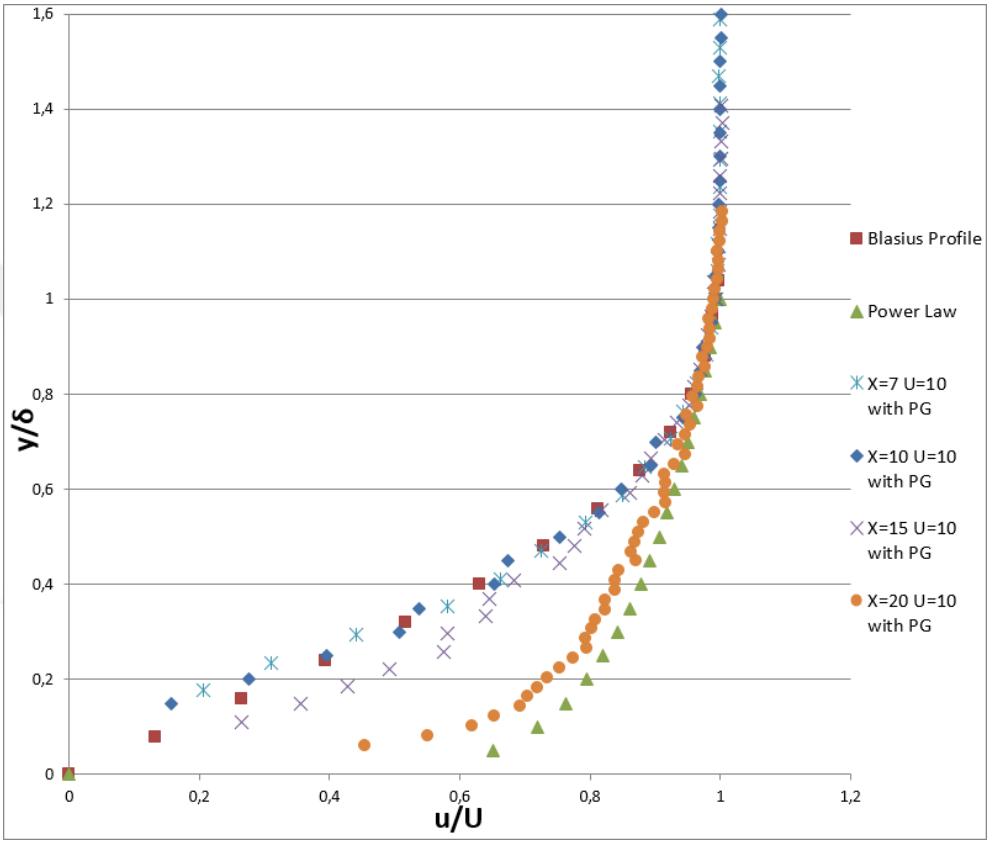

Figure 3.16 : Boundary layer profiles at x=7, x=10, x=15 and x=20 cm with pressure gradient for a flow velocity of 10 m/s.

The Tables and Figures above show the results of the pressure gradient tests at velocities of 9 and 10 m/s. According to the results, it was observed that the flow in the boundary layer was laminar up to 15 cm, but when it reached 20 cm, it was determined that the flow in the boundary layer turned into turbulence. In the base flow experiment performed at a flow velocity of 9 m/s, the boundary layer thickness at 200 mm was found to be 3.1 and the flow in the boundary layer was found to be laminar flow. According to the results of the experiment performed at the same location with pressure gradient, the delta increased to 4.7 and it was determined that the flow in the

boundary layer was turbulent. That is, the pressure gradient increases the boundary layer thickness and makes the flow turbulent after a certain position.

3.4 Experiments With Pressure Gradient And VG

While the air flow bench was under the effect of a positive pressure gradient, 10 vortex generators were placed at 5 cm and experiments were carried out.

Table 3.16 : Boundary layer thickness and flow state results of experiments performed in different locations with positive pressure gradient effect and vortex generators placed at 5 cm when flow velocity is 8.35-8.45 m/s.

X (mm)	V (m/s)	δ	Flow state	$\frac{\partial P}{\partial x}$
100	8,35	2,5	laminar flow	0,166
120	8,36	2,8	transition	0,167
130	8,34	3,4	transition	0,166
140	8,43	3,8	transition	0,169
150	8,42	4,4	turbulent flow	0,169
200	8,4	5,9	turbulent flow	0,163

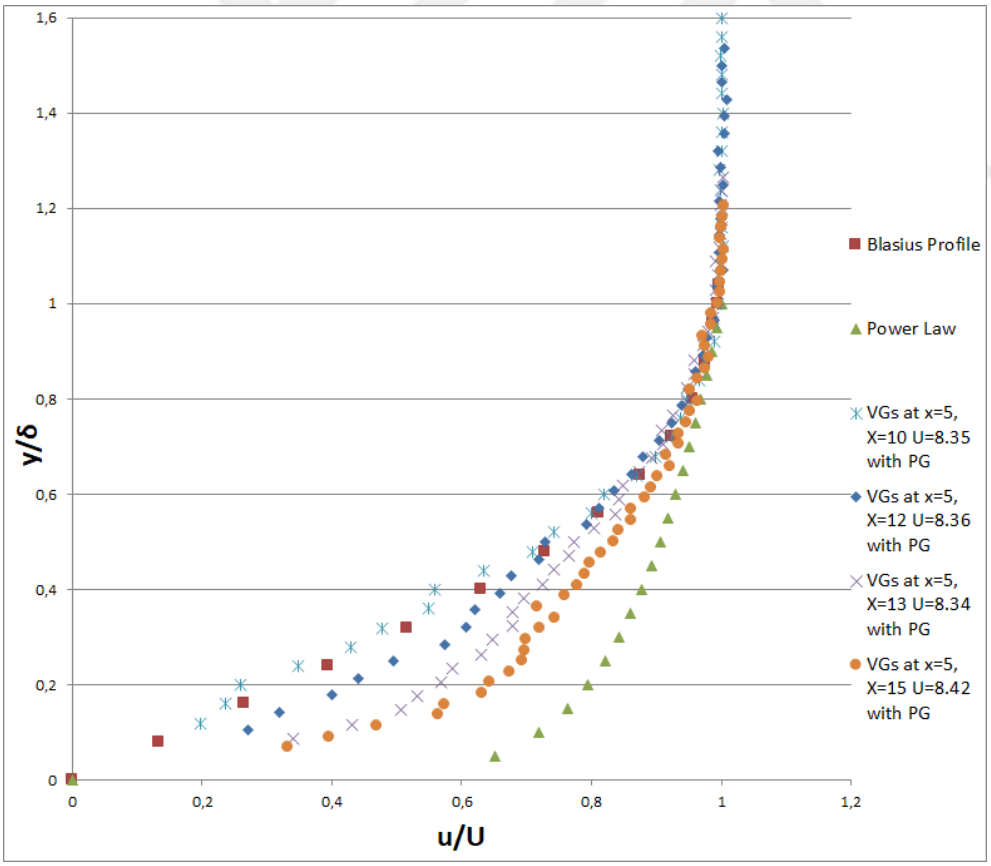

Figure 3.17 : Boundary layer profiles at x=10, x=12, x=13 and x=15 cm with pressure gradient and vortex generators for a flow velocity of 8.35-8.45 m/s.

Table 3.17 : Boundary layer thickness and flow state results of experiments performed in different locations with positive pressure gradient effect and vortex generators placed at 5 cm when flow velocity is 9 m/s.

X (mm)	V (m/s)	δ	Flow state	$\frac{\partial P}{\partial x}$
90	9,02	2,3	laminar flow	0,194
100	9,05	2,6	transition	0,194
120	9,03	3,4	transition	0,195
150	9	4,7	turbulent flow	0,193

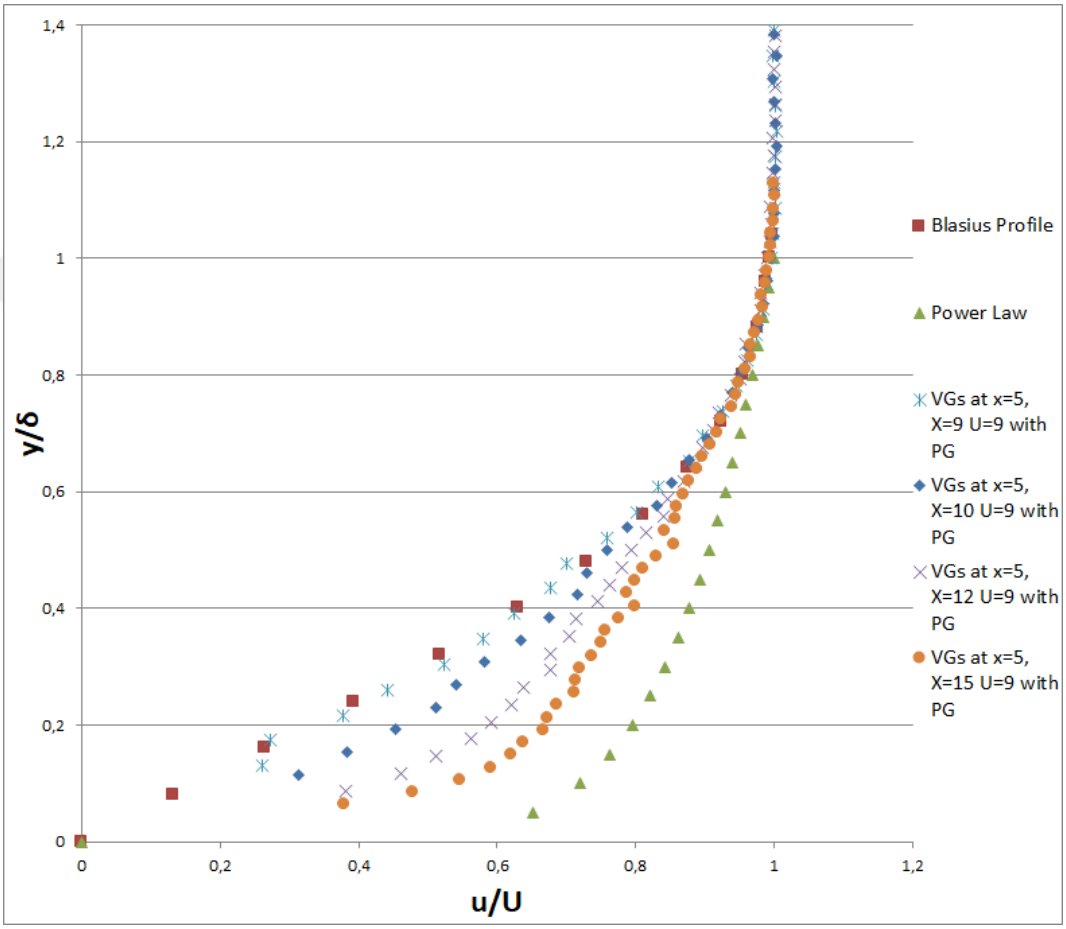

Figure 3.18 : Boundary layer profiles at x=9, x=10, x=12 and x=15 cm with pressure gradient and vortex generators for a flow velocity of 9 m/s.

The 3.17 table and graph above show the results of pressure gradient experiments with vortex generators placed at 5 cm at a flow velocity of 9 m/s. According to the results obtained, it has been determined that the flow in the boundary layer is in the transition zone at 12 cm, but when it reaches 15 cm, the flow in the boundary layer turns into turbulence.

Table 3.18 : Boundary layer thickness and flow state results of experiments performed in different locations with positive pressure gradient effect and vortex generators placed at 5 cm when flow velocity is 10 m/s.

X (mm)	V (m/s)	δ	Flow state	$\frac{\partial P}{\partial x}$
70	10,12	1,8	laminar flow	0,246
80	10,15	2	laminar flow	0,246
100	10,07	2,7	transition	0,245
150	10,11	4,5	turbulent flow	0,246

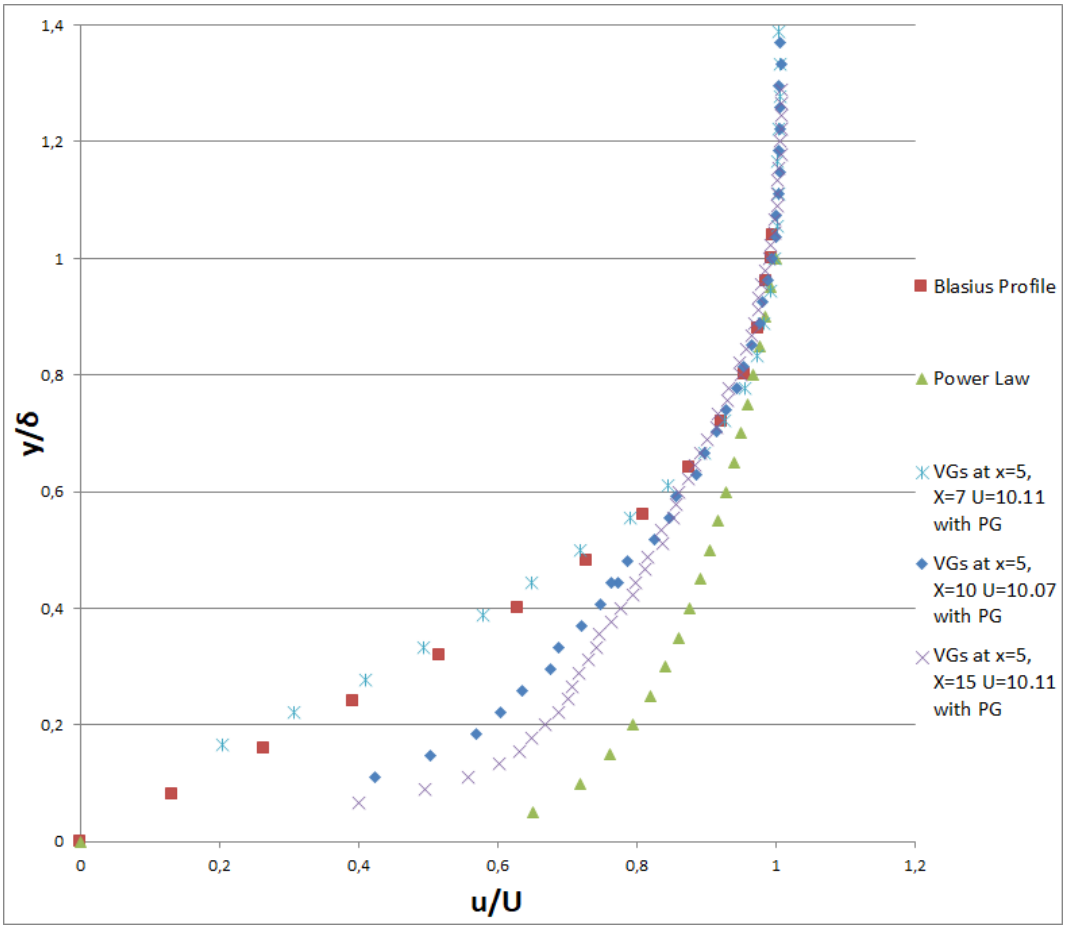

Figure 3.19 : Boundary layer profiles at x=7, x=10 and x=15 cm with pressure gradient and vortex generators for a flow velocity of 10 m/s.

The 3.18 table and graph above show the results of pressure gradient experiments with vortex generators placed at 5 cm at a flow velocity of 10 m/s. According to the results obtained, it has been determined that the flow in the boundary layer is in the transition zone at 10 cm, but when it reaches 15 cm, the flow in the boundary layer turns into turbulence.

3.5 Comparison Of Experiments

In this section, the results of the experiments with and without a vortex generator, the experiments with and without a pressure gradient will be compared at many velocities. At the same time, graph with delta and Re number results are shown below. Let's start by comparing empty flat plate experiments at the same location at different speeds.

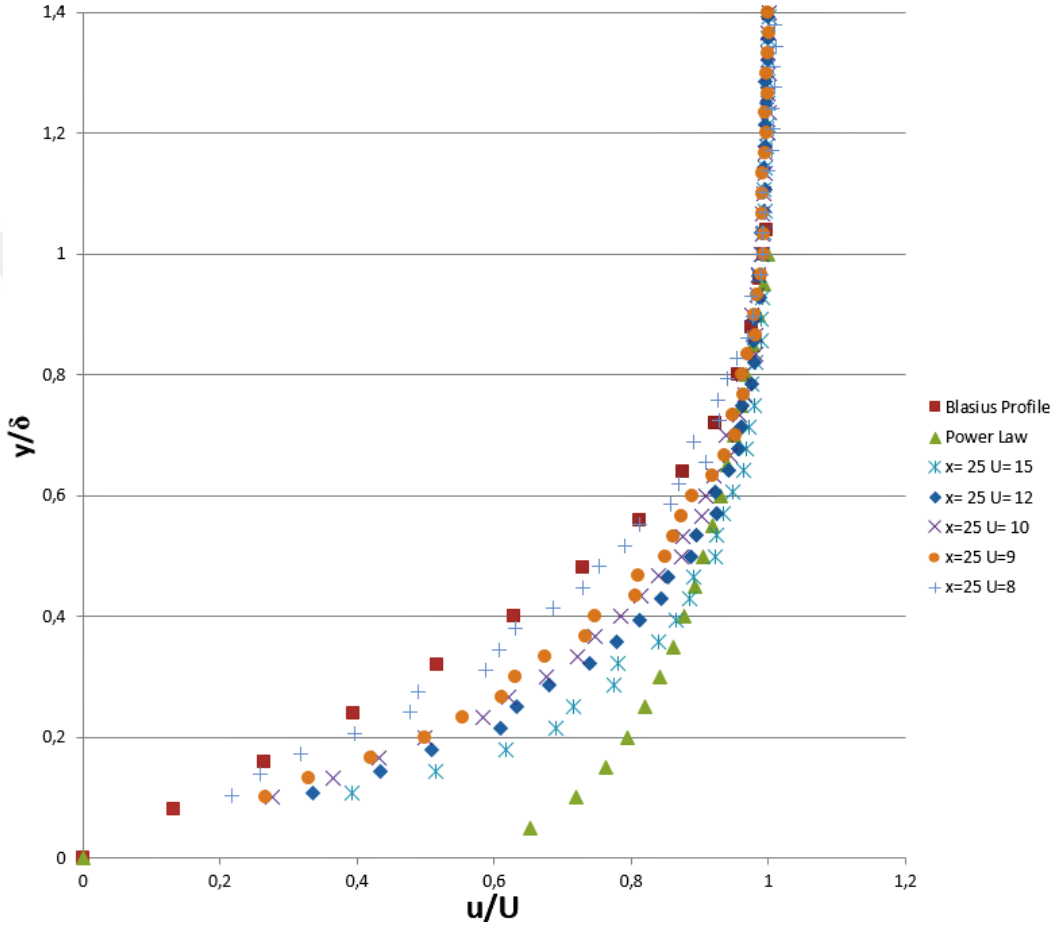

Figure 3.20 : Boundary layer profiles at x=25 cm for 8,9,10,12 and 15 m/s flow velocities.

The boundary layer profiles are compared to the Blasius solution of laminar boundary layer or power law of turbulent boundary layer, normalized by boundary layer thickness and free-stream velocity. The experiments in the Figure 3.20 were performed using a blank plate. No vortex generators or parts to create a pressure gradient were used. The test results at the same position at different speeds are compared in the graph. As a result, it has been shown that the transition region moves upstream as

the free stream velocity increases. Boundary layer on flat plate remains completely laminar at low free-stream velocities.

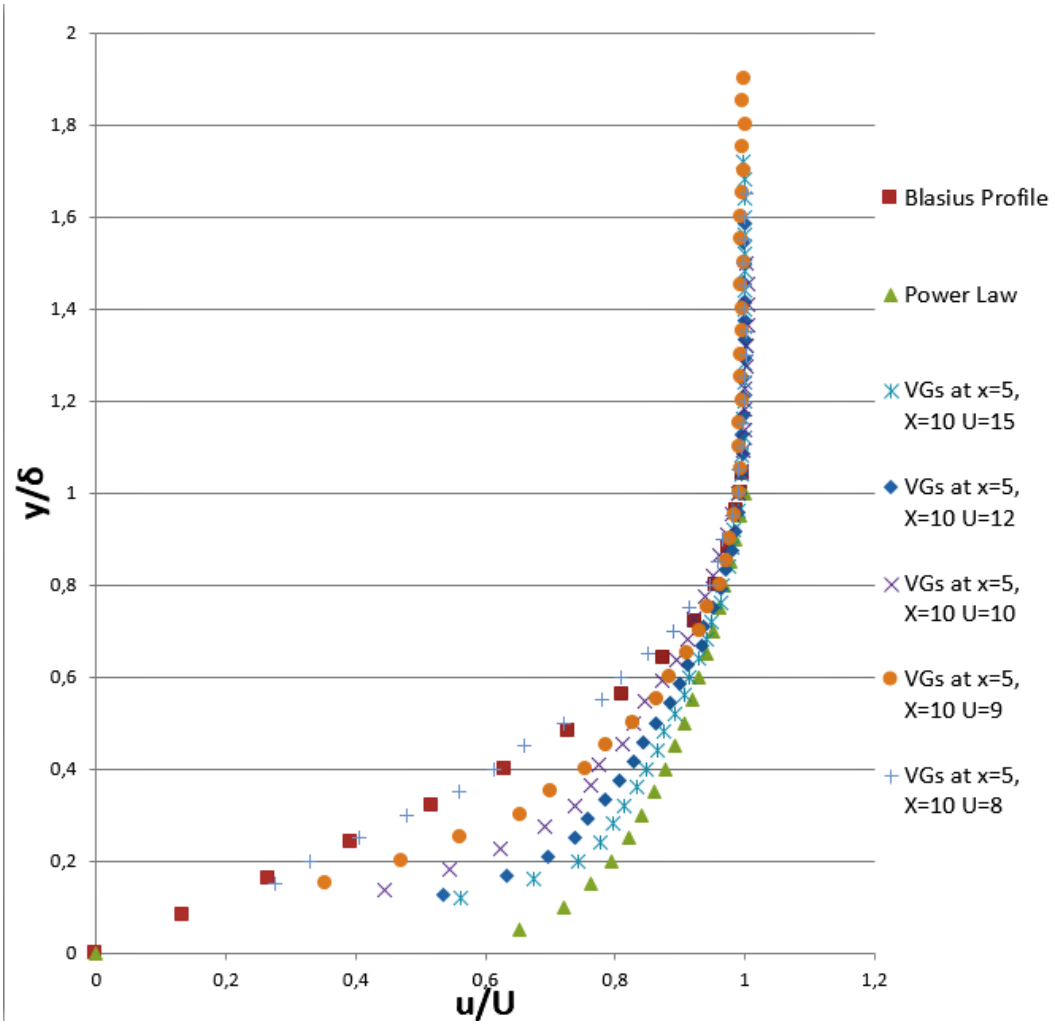

Figure 3.21 : Boundary layer profiles for 8,9,10,12 and 15 m/s flow velocities at x=10 cm with vortex generators at x=5 cm.

In Figure 3.21, boundary layer profiles at 10 cm from the leading edge are presented at various free stream velocities of 8, 9, 10, 12, and 15 m/s while the vortex generators were placed at 5 cm on the flat plate. As can be seen from the Figure laminar velocity profiles exists downstream of the VG's at 8 m/s free stream velocity. Laminar region always occurs in the vicinity of VGs, however its length diminishes with increasing Re number. Hence, as the free-stream velocity is increased, the boundary layer profiles approaches fully developed turbulent profiles. In the experiment where the flow velocity was 15 m/s, transition region is already completed and turbulent boundary layer properties are acquired at downstream positions.

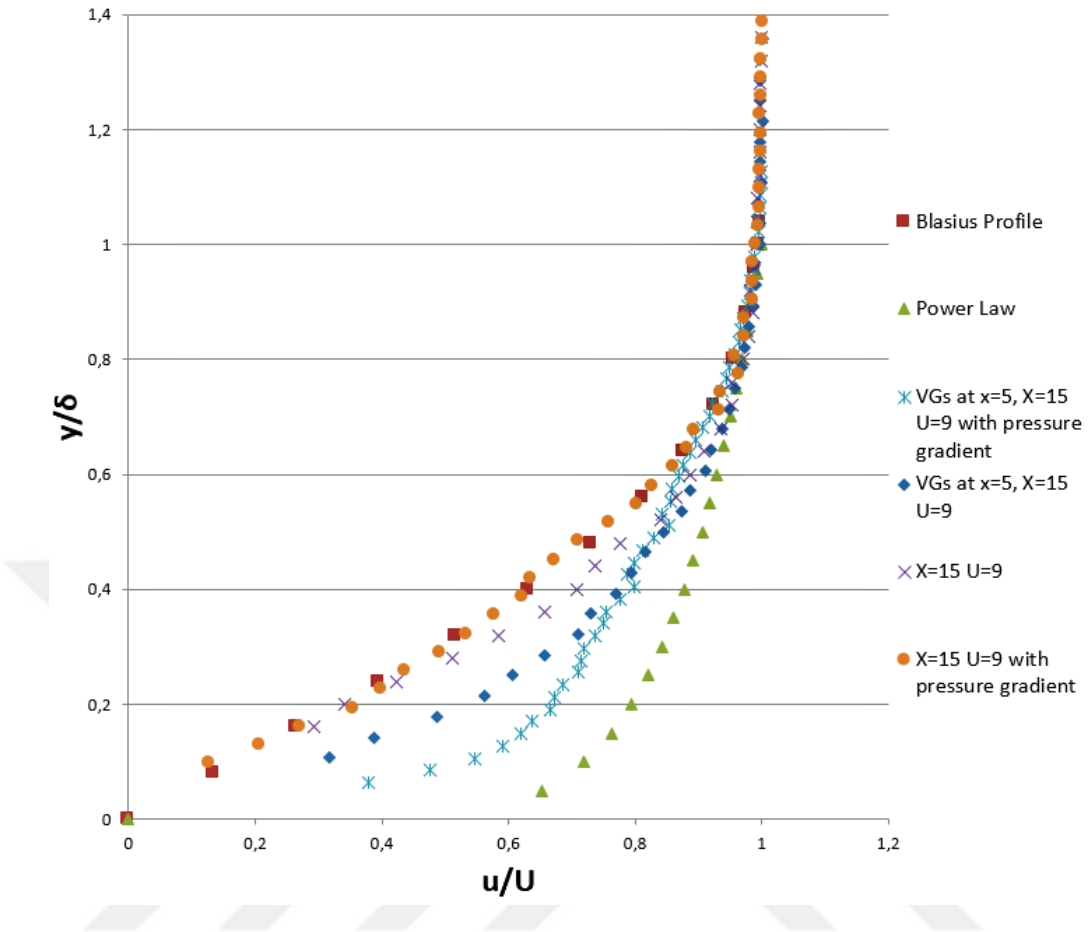

Figure 3.22 : Boundary layer profiles of experiments with vortex generator, without vortex generator, with and without pressure gradient when flow velocity is 9 m/s at X=15 cm.

In Figure 3.22, experiments with and without pressure gradient were performed when the vortex generators were at 5 cm on the flat plate. In addition, experiments with and without pressure gradient without vortex generator were taken and all these boundary layer profiles were compared in this graph. All experiments in this graph were performed at a flow rate of 9 at 15 cm. When we look at the experiments without vortex generator, it is understood that the boundary layer flow in the two experiments is laminar or at the beginning of the transition zone. When the experiments without the vortex generator are compared, it is seen that the pressure gradient does not have much effect on the flow in the boundary layer, but the delta was found to be 2.5 in the empty plate experiment shown in Table 3.2, and it was found to be 3.1 in the pressure gradient experiment as shown in Table 3.14. In other words, it has been determined that

the positive pressure gradient increases the boundary layer thickness. When we look at the vortex generator experiments, it is determined that the pressure gradient experiment is more linear than without pressure gradient experiment, and the flow in the boundary layer is very close to turbulence. As seen in the graph, the result of the experiment with the vortex generator was more turbulent than the result of the experiment without the vortex generator. This result shows that the flow in the boundary layer causes faster turbulence thanks to the vortex generator.

3.5.1 Boundary layer thickness development along the free stream direction graphs

Development of the boundary layer thickness (δ) along the flat plate for controlled and uncontrolled flow states is shown in the graphs below. These graphs are the results of experiments performed at free stream velocities of 8,9,10,12 and 15 m/s. Results are compared with Blasius solution.

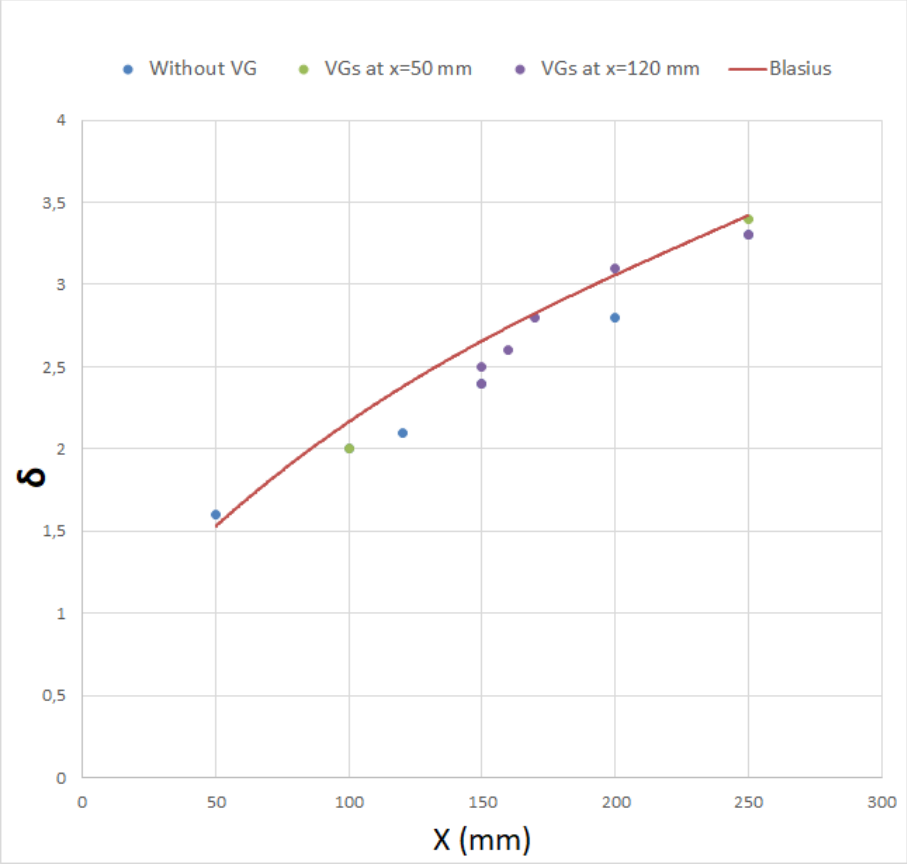

Figure 3.23 : Boundary layer thickness (δ) versus downstream positions(x) from leading edge with and without a vortex generator, free-stream velocity is 8 m/s

In Figure 3.23, boundary layer thickness (δ) versus downstream positions(x) from leading edge with and without a vortex generator, free-stream velocity is 8 m/s. It has been shown that the flow in the boundary layer is laminar since experimental results without a vortex generator overlap with the theoretical calculations. Controlled flow with vortex generators placed at 50 mm, it seems to be the transition started at 250 mm according to Figure 3.22. In the results of the experiments with the vortex generators placed at 120 mm, it is seen that the flow is affected by the generators and remained laminar up to the end of the investigation region.

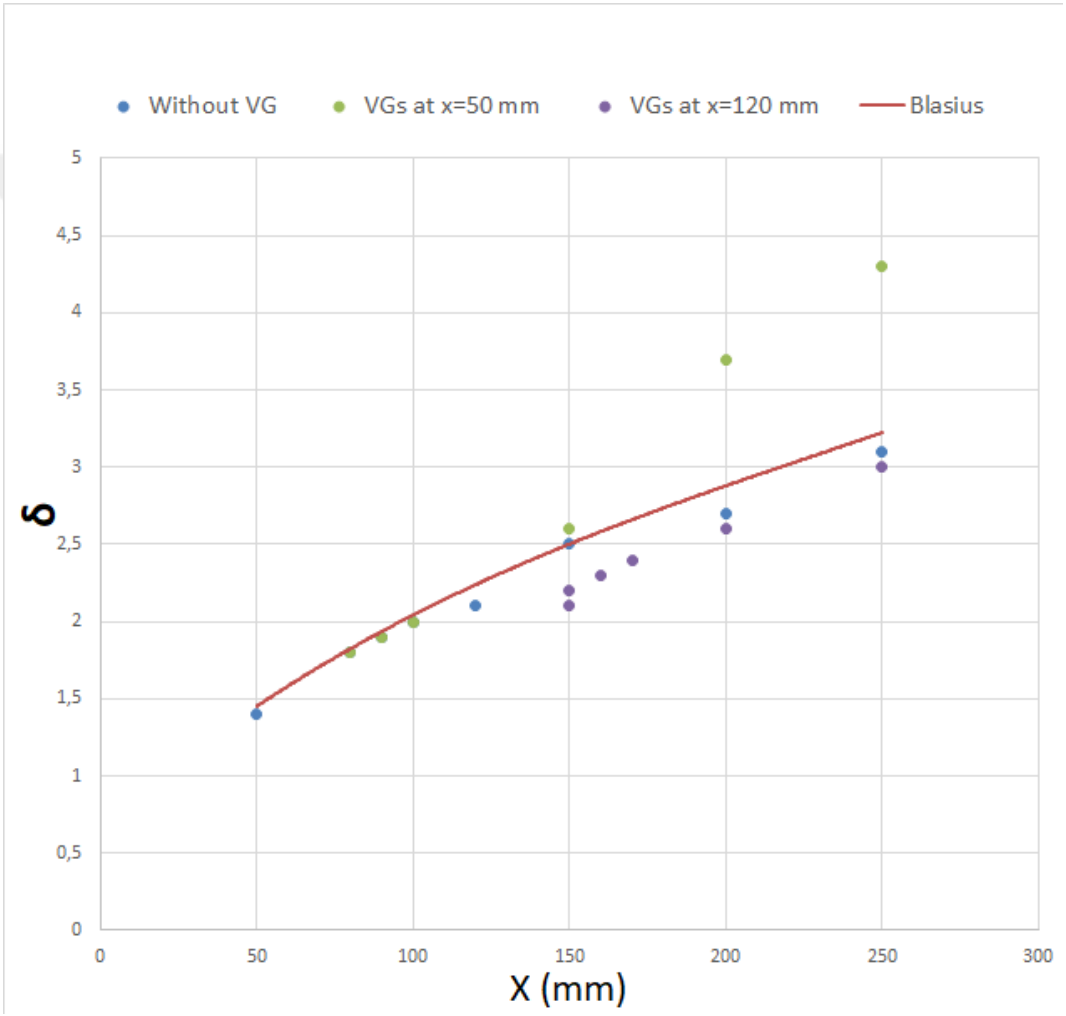

Figure 3.24 : Boundary layer thickness (δ) versus downstream positions(x) from leading edge with and without a vortex generator, free-stream velocity is 9 m/s

Figure 3.24 shown that the flow in the boundary layer is laminar since experimental results without a vortex generator overlap with the theoretical calculations. Controlled flow with vortex generators placed at 50 mm, at 150 mm according to Figure 3.24 the

flow in the boundary layer appears to be in the transition zone. According to Figure 3.24, the flow appears to be laminar up to 100 mm in the experiments performed when the free flow velocity is 9 m/s with vortex generators placed at 50 mm. In the results of the experiments with the vortex generators placed at 120 mm, it is seen that the flow is affected by the generators and remained laminar up to the end of the investigation region.

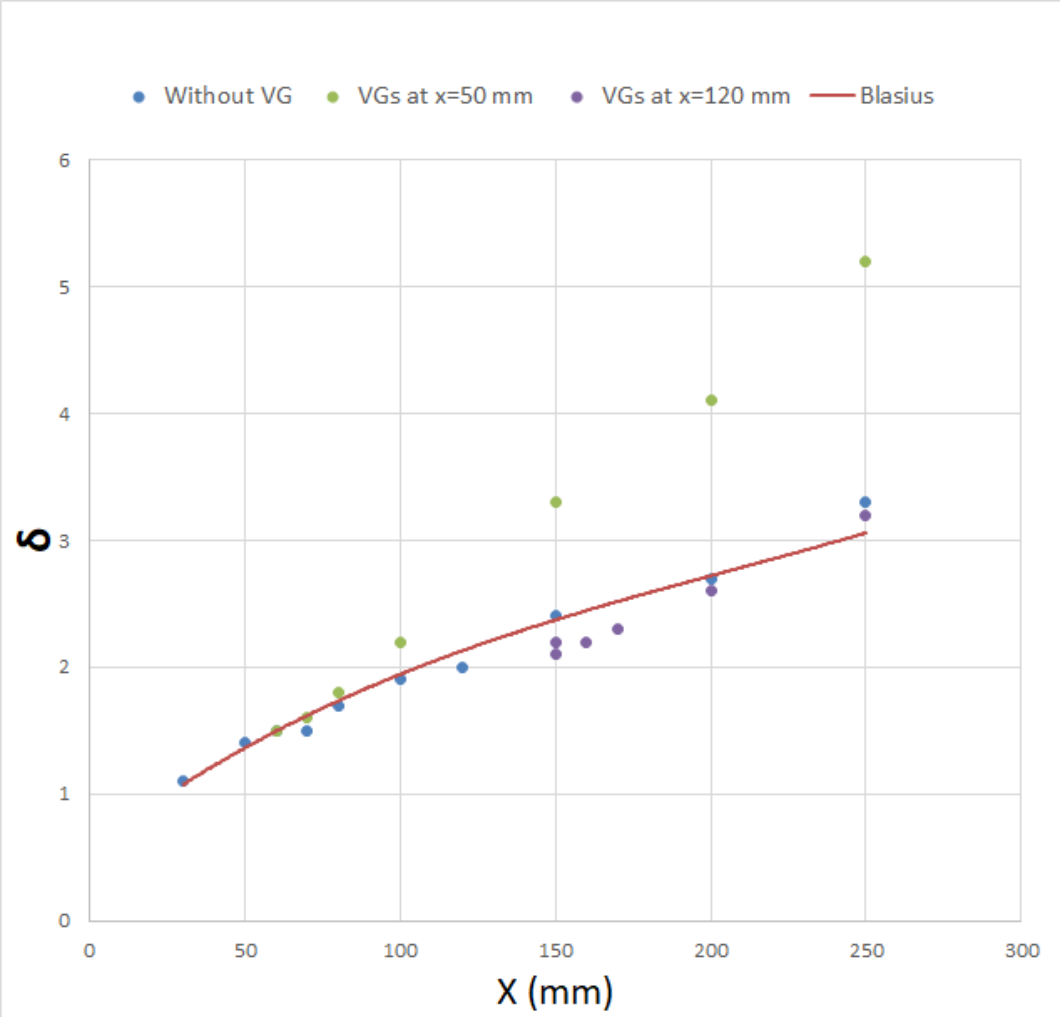

Figure 3.25 : Boundary layer thickness (δ) versus downstream positions(x) from leading edge with and without a vortex generator, free-stream velocity is 10 m/s

Development of the boundary layer thickness (δ) along the flat plate for the controlled and uncontrolled flow conditions of the experiments performed at a free stream velocity of 10 m/s is shown in Figure 3.25. The flow in the boundary layer is shown to be laminar, since the results of the experiments without vortex generators agree with the theoretical calculations. Controlled flow with vortex generators placed at 50 mm,

it seems to be the transition started at 80 mm according to Figure 4. In the results of the experiments with the vortex generators placed at 120 mm, it is seen that the flow is affected by the generators and remained laminar up to the end of the investigation region.

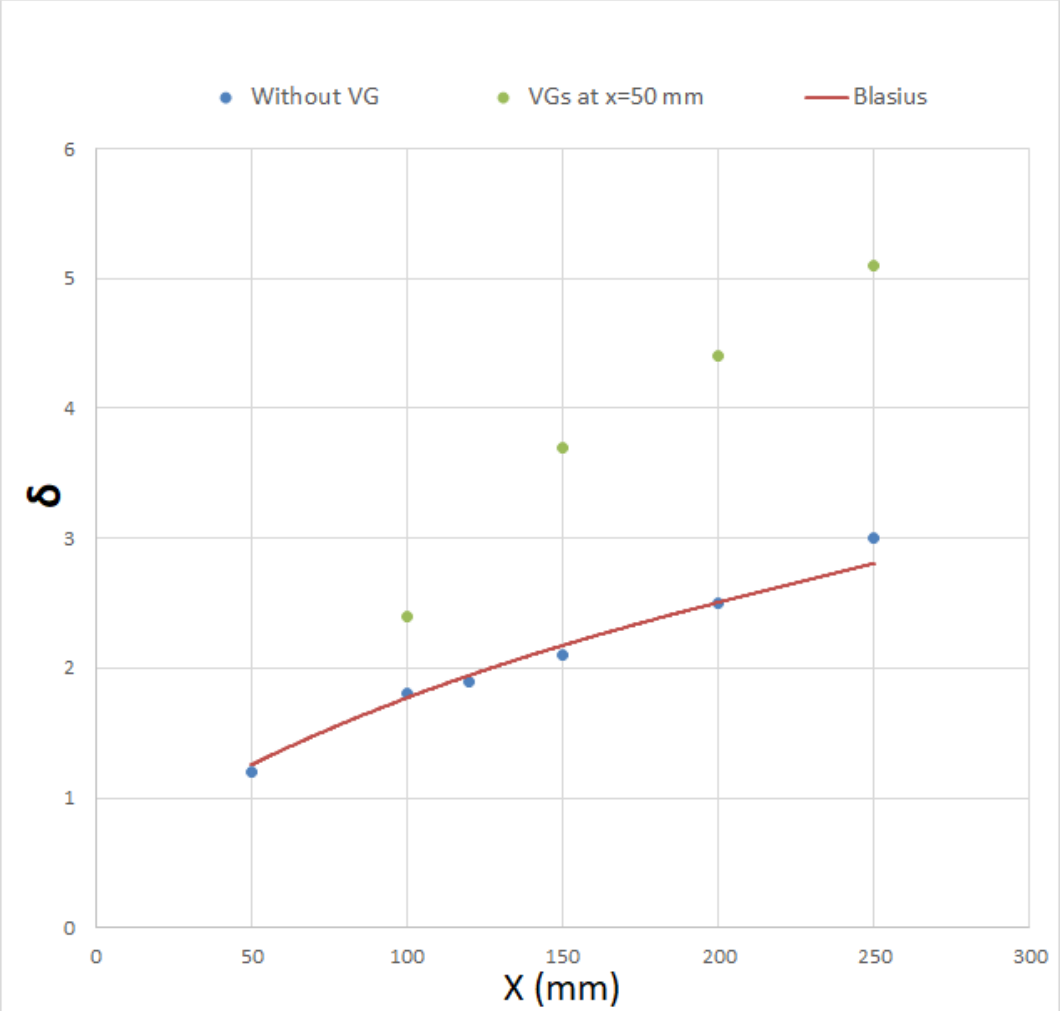

Figure 3.26 : Boundary layer thickness (δ) versus downstream positions(x) from leading edge with and without a vortex generator, free-stream velocity is 12 m/s

The evolution of the boundary layer thickness (δ) along the flat plate according to the results of the experiments with and without the vortex generator, performed at a free stream velocity of 12 m/s, is shown in Figure 3.26. The flow in the boundary layer has been shown to be laminar up to 25 cm, which is compatible with theoretical calculations, according to the results of experiments without vortex generators. According to Figure 3.26, it has been determined that the flow in the boundary layer at 25 cm is in the transition region.

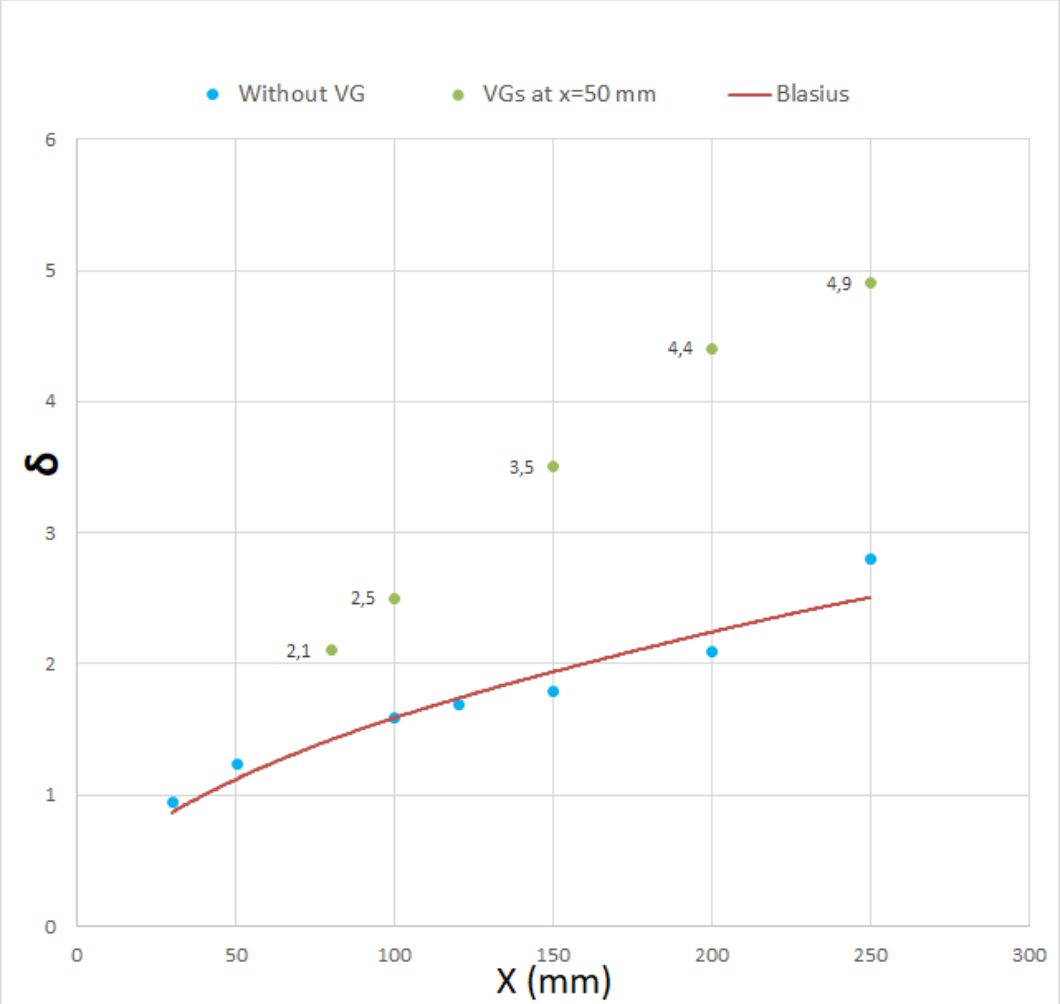

Figure 3.27 : Boundary layer thickness (δ) versus downstream positions(x) from leading edge with and without a vortex generator, free-stream velocity is 15 m/s

The evolution of the boundary layer thickness (δ) along the flat plate according to the results of the experiments with and without the vortex generator, performed at a free stream velocity of 15 m/s, is shown in Figure 3.27. According to Figure 3.27, it is shown that the flow in the boundary layer is laminar up to 20 cm and turns into turbulence at 25 cm, which is consistent with the theoretical calculations according to the results of the experiments performed without vortex generators. According to the results of all vortex generator experiments in this figure, it is seen that the flow in the boundary layer is turbulent.

The variation of the boundary layer thickness to position ratio (δ/x) along the flat plate with respect to the Reynolds number for controlled and uncontrolled flow conditions is shown in the graphs below. These graphs are the results of the experiments performed

at free flow velocities of 8,9,10,12 and 15 m/s. The results are compared with the Blasius solution.

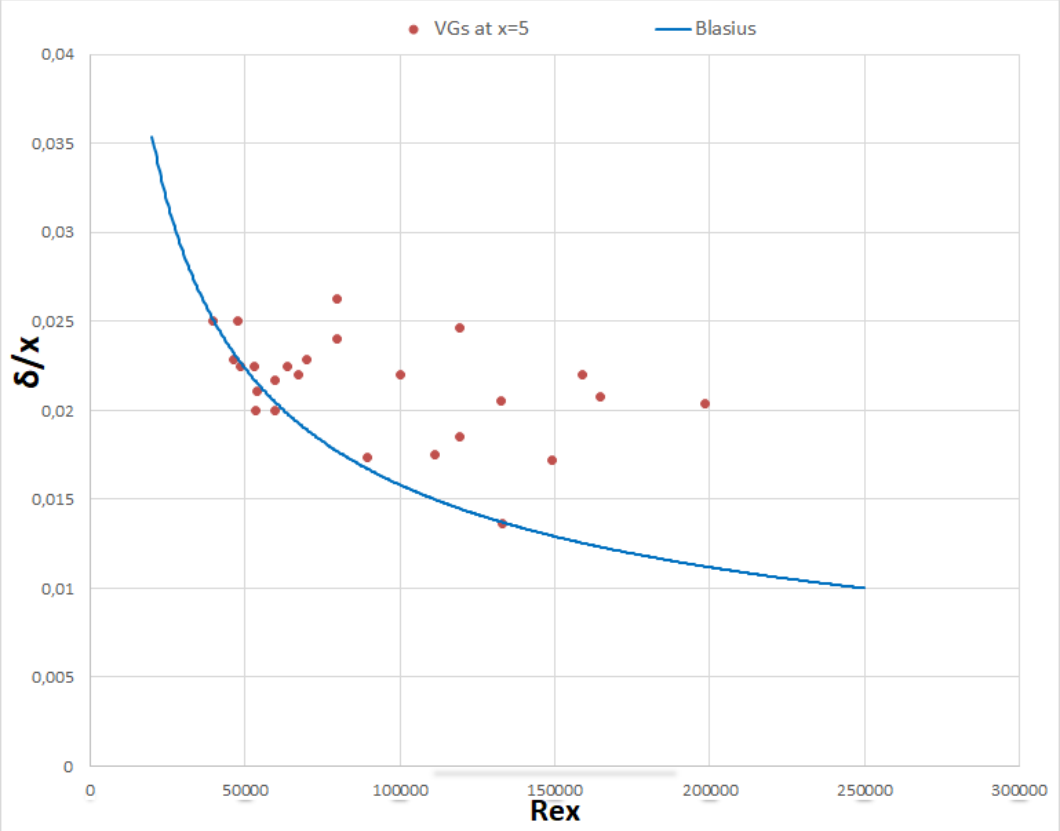

Figure 3.28 : Reynolds number (Re) versus boundary layer thickness to positions ratio (δ/x) from leading edge

Figure 3.28 shows the graph of boundary layer thickness to position ratio comparison with Reynolds number of the experiments performed with the vortex generators placed at 5 cm at different velocities. As seen in the graph, the results of several of the experiments are consistent with the theoretical calculations, namely around the Blasius curve, and the boundary layer profiles of these experiments also show that the flow is laminar. In the experiments, the vortex generators increase the boundary layer thickness, so the ratio δ/x increases and as a result the points appear on the curve in the graph. In the results of the experiments of many of the points appearing on this curve, it is seen that the flow in the boundary layer is turbulent. It is confirmed with this graph that the flow in the boundary layer is in the transition zone only at points close to the curve above the curve.

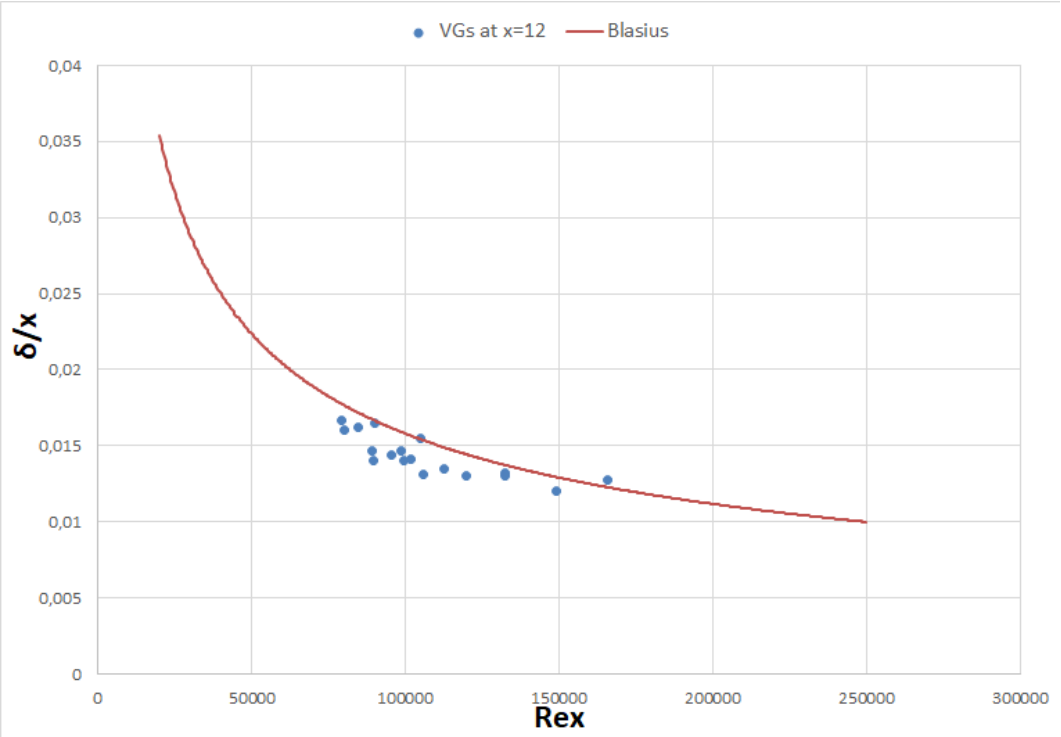

Figure 3.29 : Reynolds number (Re) versus boundary layer thickness to positions ratio (δ/x) from leading edge

Figure 3.29 shows the graph of boundary layer thickness to position ratio comparison with Reynolds number of the experiments performed with the vortex generators placed at 12 cm at different velocities. As seen in the graph, the results of several of the experiments are consistent with the theoretical calculations, namely around the Blasius curve, and the boundary layer profiles of these experiments also show that the flow is laminar or transition.

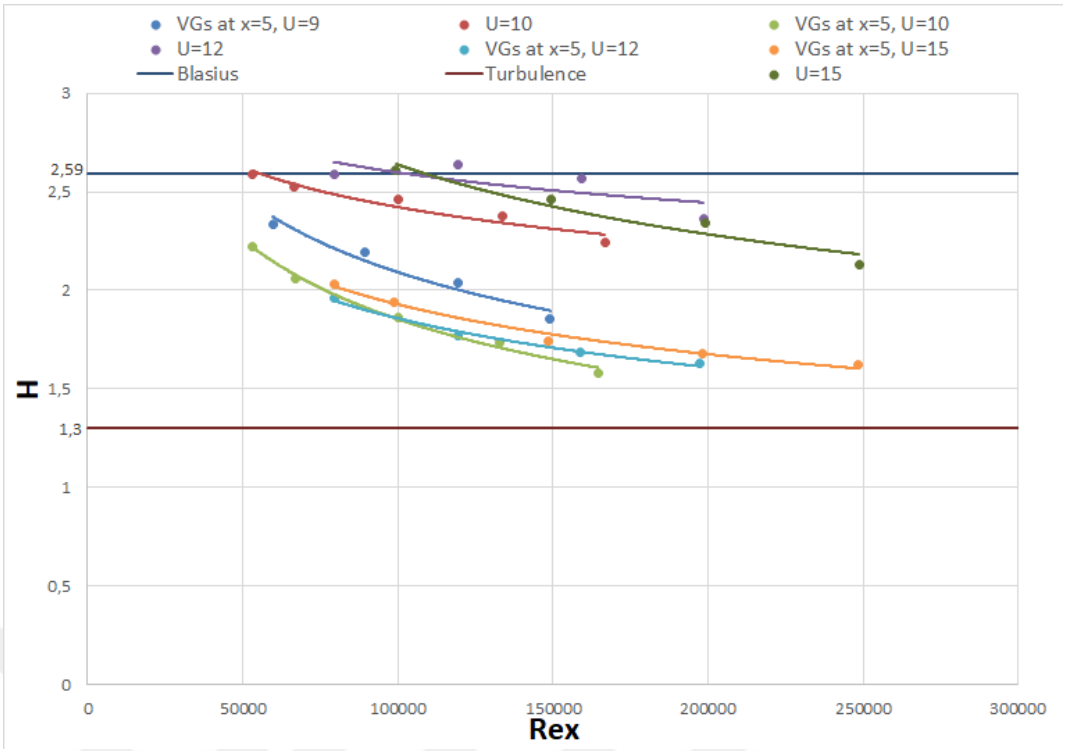

Figure 3.30 : Reynolds number (Re) versus Shape factor (H=δ/θ)

Figure 3.30 shows the graph of shape factor (H) comparison with Reynolds number of the experiments performed with and without a vortex generator at different velocities. As seen in the graph, the results of a few of the experiments are consistent with the theoretical calculations, namely around the Blasius line, and the boundary layer profiles of these experiments also show that the flow is laminar. The experimental results of points close to the Blasius line are theoretically consistent because the boundary layer profiles of these experiments also show that the flow is in the transition zone. The Shape factor (H) results of the vortex-generator experiments are closer to the turbulence line than the ones without vortex generator, and the boundary layer profiles of the vortex-generator experiments already show turbulent flow in many locations.

3.6 Power Spectrum Measurements Results

In the following, we will discuss the measurements of velocity downstream and the effect of vortex generators on it with hot-wire probe. Here we will show time signals and spectra obtained by hot wire probe measurements at different y-positions.

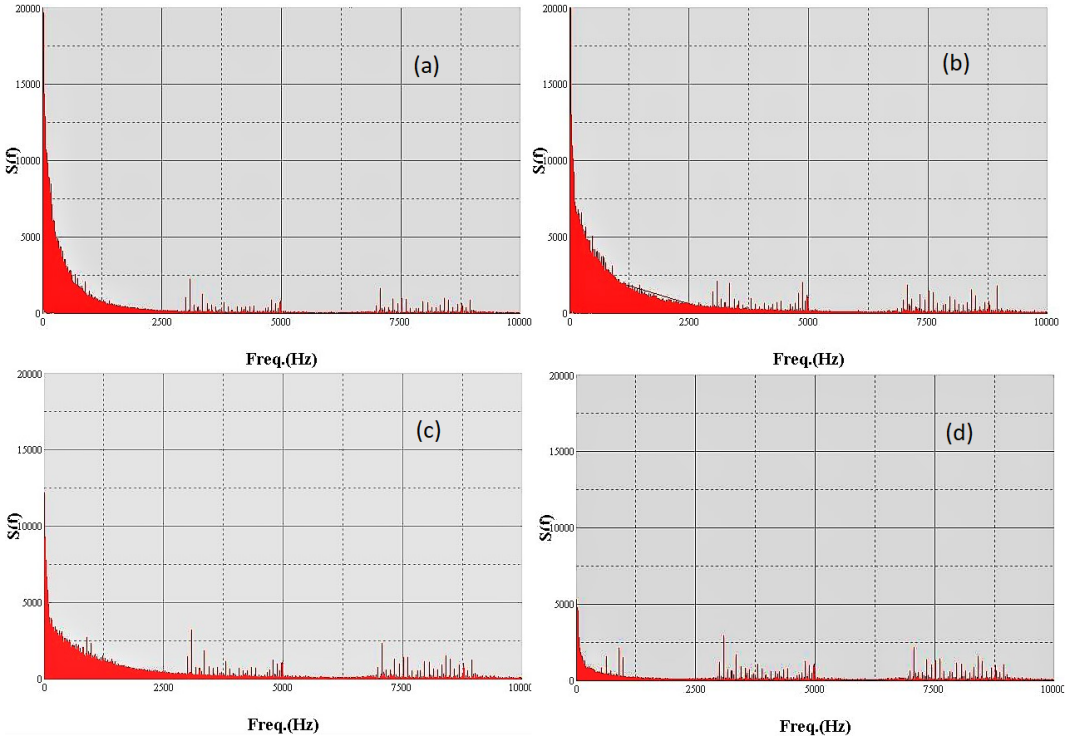

Figure 3.31 : Hot-wire measurements at U= 10 m/s and x= 25 cm with vortex generators placed at 5 cm. The corresponding spectra (a) y/δ = 0.0192, (b) y/δ= 0.307, (c) y/δ= 0.596, (d) y/δ= 0.884.

Figure 3.31 shows the spectra obtained at the 4 different distance from the flat plate (y position) where the largest y is in the boundary layer edge and the others are scattered throughout the boundary layer. This experiment was performed at 200 mm behind the vortex generators at a free stream velocity of 10 m/s with vortex generators placed at 50 mm. And according to the results of the experiment with the pitot tube at this location, it was determined that the flow is turbulent in the boundary layer profile. As can be seen, the character of the spectrum changes significantly as it approaches the plate, and it can be clearly seen that low frequency content increases and high frequency content decreases compared to boundary layer edge.

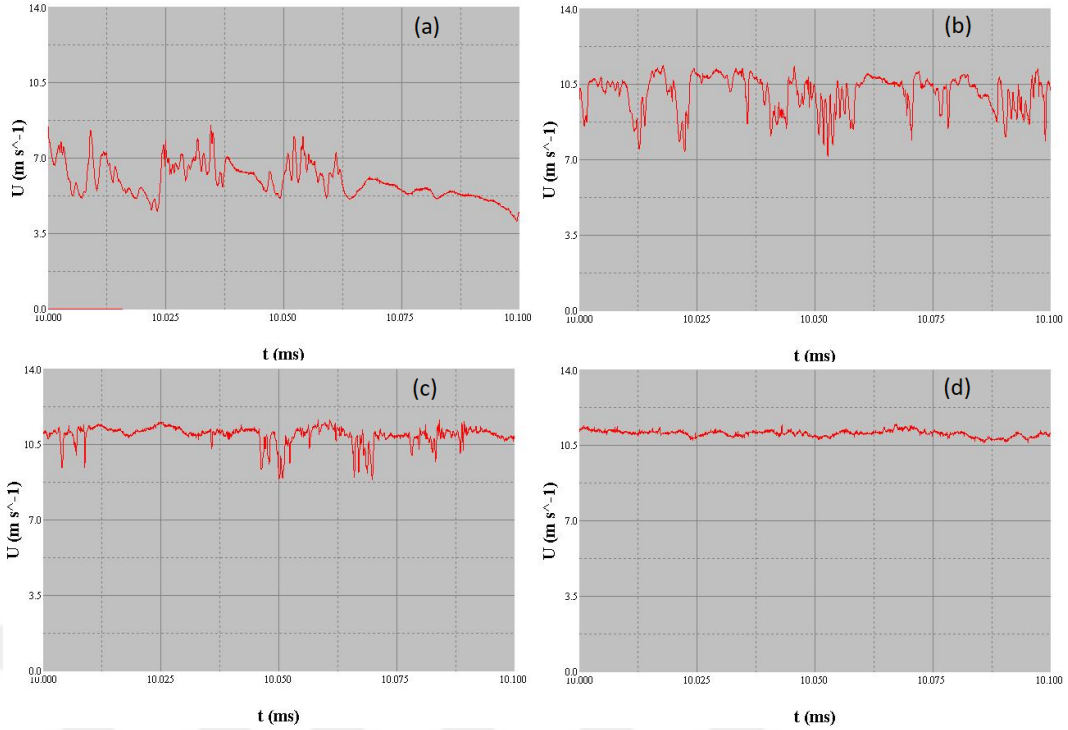

Figure 3.32 : Hot-wire measurements at U= 10 m/s and x= 25 cm with vortex generators placed at 5 cm. Time signals from 3 different heights inside the boundary layer and one in the free stream; (a) y/δ = 0.0192, (b) y/δ= 0.307, (c) y/δ= 0.596, (d) y/δ= 0.884.

Figure 3.32 shows the time signals obtained at the 4 different distance from the flat plate (y position) where the largest y is in the boundary layer edge and the others are scattered throughout the boundary layer. This experiment was performed at the same locations as the experiments in Figure 3.30. And according to the results of the experiment with the pitot tube at this location, it was determined that the flow is turbulent in the boundary layer profile. As can be seen, the character of the signals changes significantly as it approaches the plate. It has been determined that the turbulence intensity near the surface is high as seen in the graphs a and b, while it decreases as it moves away from the plate. In other words, it is seen that the intensity approaches the free stream turbulence intensity as it moves away from the surface.

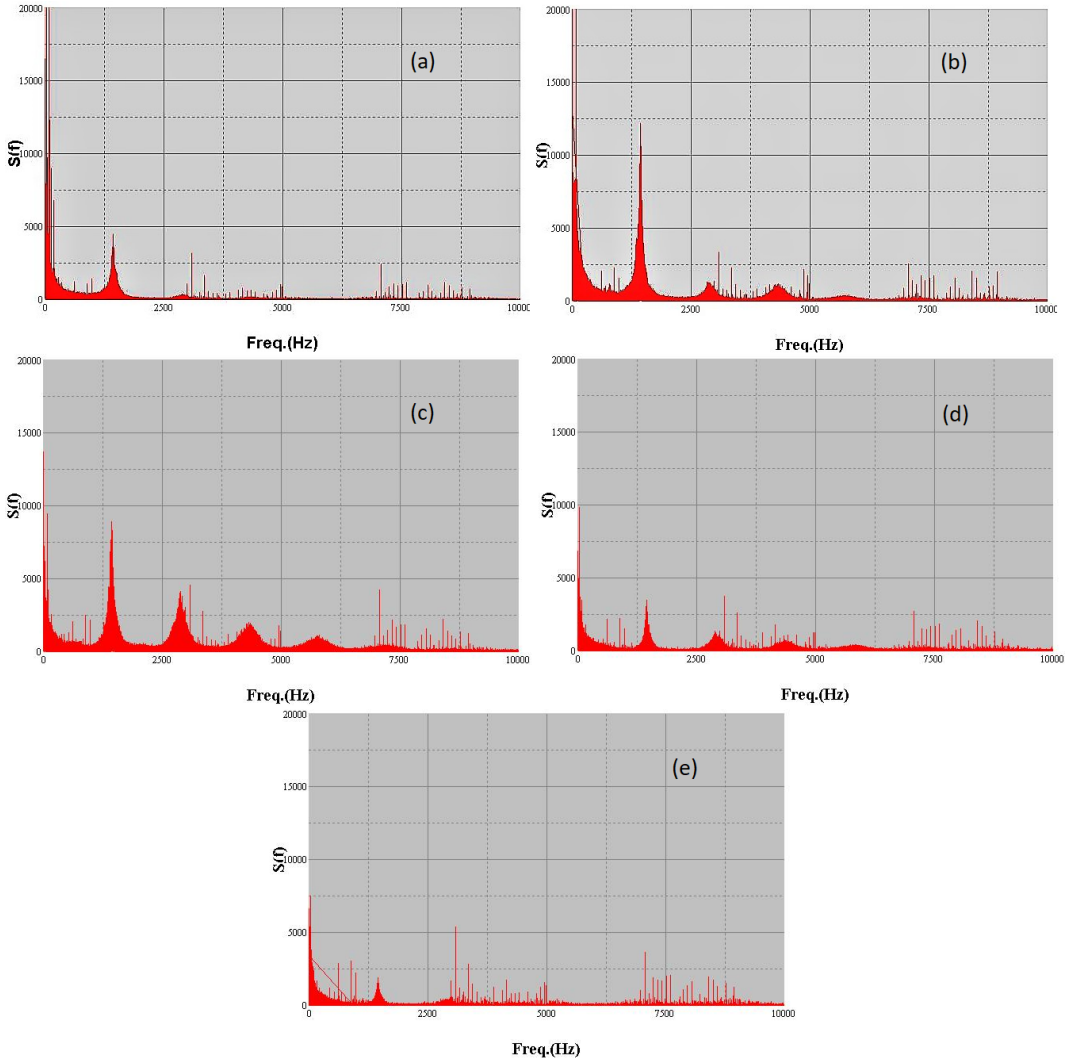

Figure 3.33 : Hot-wire measurements at U= 10 m/s and x= 6 cm with vortex generators placed at 5 cm. The corresponding spectra (a) y/δ = 0.067, (b) y/δ= 0.4, (c) y/δ= 0.73, (d) y/δ= 1.06 (e) y/δ = 1.312.

Figure 3.33 shows the time signals obtained at the 5 different distance from the flat plate (y position) where the largest y is in the free stream and the others are scattered throughout the boundary layer. These experiments were performed at 60 mm and a free stream velocity of 10 m/s with vortex generators positioned at 50 mm. And the result of the boundary layer profile at this location shows that the flow in the boundary layer is laminar. It has been confirmed that the flow at this location is laminar with Reynolds and boundary layer thickness graphs. Looking at Figure 3.33, the effective frequency modes created by the vortex generators are seen, and the modes that increased up to the y position in the c graph started to disappear after this position.

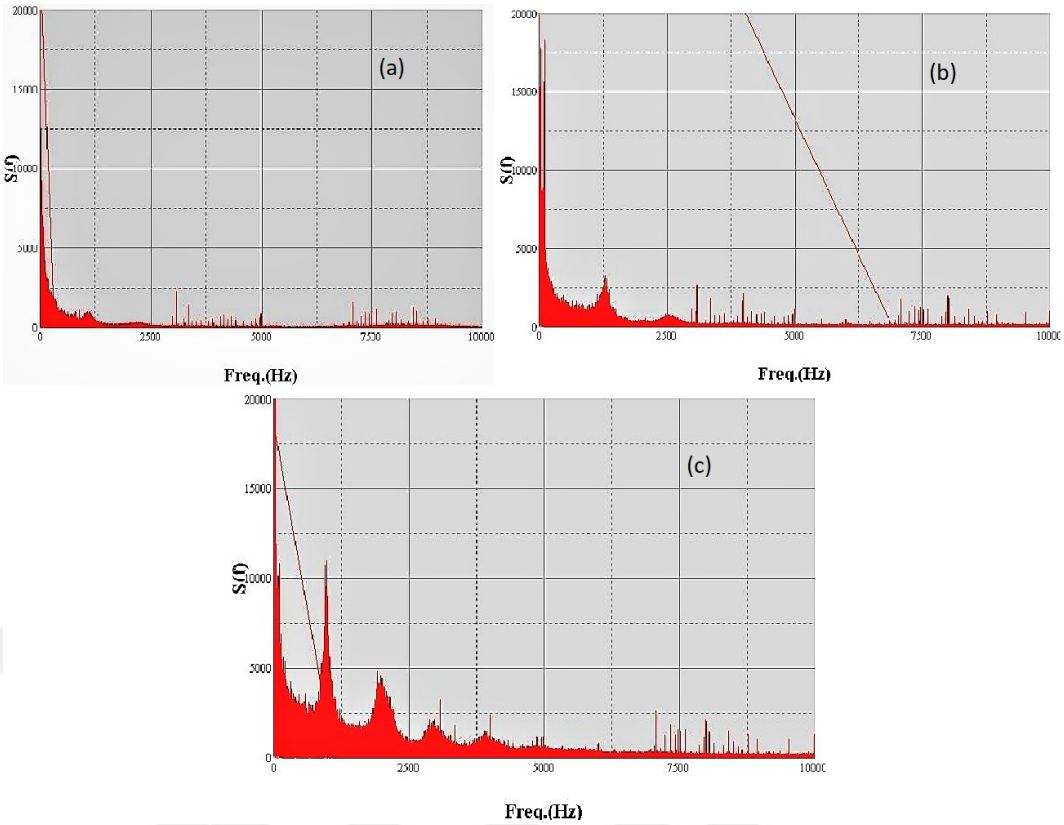

Figure 3.34 : Hot-wire measurements at x= 6 cm with vortex generators placed at 5 cm. Time signals from 4 different heights inside the boundary layer; (a) U= 9 m/s y/δ = 0.062, (b) U= 10 m/s y/δ= 0.064, (c) U= 12 m/s y/δ= 0.067.

Figure 3.34 shows the spectral obtained at the same y position in the boundary layer at 3 different free stream velocities. This experiment was performed at 60 mm at free stream velocities of 9, 10 and 12 m/s with vortex generators placed at 50 mm. Experiments were carried out by aligning the hot wire probe with a vortex generator. As a result, while the vortex generator does not seem to have an effect on the spectrum graph at 9 m/s free stream velocity, the effect of the vortex generators began to appear as the velocity increased. In other words, as the speed increases, the number of effective frequency modes also increases.

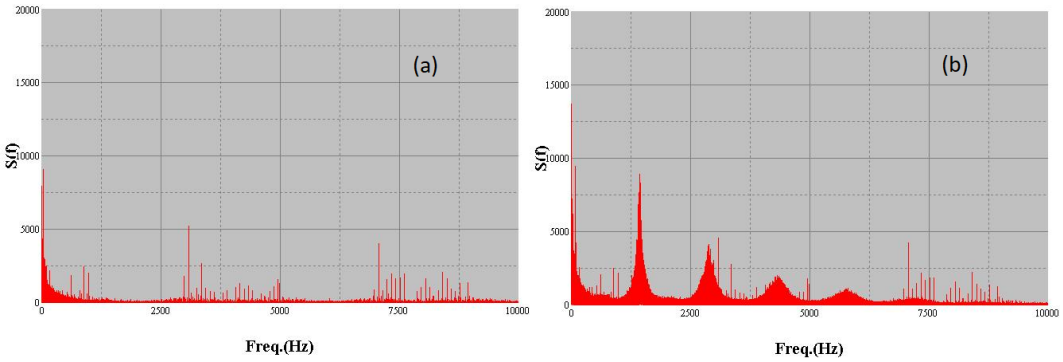

Figure 3.35 : Hot-wire measurements at U= 10 m/s and x= 6 cm with vortex generators placed at 5 cm. The hot-wire probe is aligned (a) in the middle of the two vortex generators, (b) with one vortex generator.

Figure 3.35 shows the spectral results of experiments with the hot wire probe aligned with the vortex generator and aligned in the middle of the two vortex generators. These two experiments were performed at 60 mm and a free stream velocity of 10 m/s with vortex generators positioned at 50 mm. And the distance from the probe to the plate was the same in both experiments as y/δ= 0.73. Also, at this location where we did the experiment, the y/h value is 1.1. Looking at the figure, there are 5 active frequency modes in the b graph and their intensity is gradually decreasing. However, the mode does not appear at all in the graph a. As a result, it has been determined that the vortex generator has a great effect on the trace regions of the flow in the boundary layer, which can be seen in the power spectrum results.

4. CONCLUSIONS

In this thesis, boundary layer transition by means of vortex generators is investigated experimentally. Vortex generators have many different uses, they are to prevent flow separation, control the separated flow, delay the transition of flow to turbulence, reduce drag in cars, etc. The purpose of using vortex generators in this study is to explain in detail how they affect the flow in the boundary layer.

First of all, the studies in the literature were scanned and the vortex generators used and the transition from laminar to turbulent flow in the boundary layer were examined in detail. In line with the researches, a spherical ball with a diameter of 1 mm was chosen as the vortex generator. Experiments with and without a vortex generator were performed and the boundary layer flow under investigation was subjected to a positive pressure gradient and these experiments were compared. Experiments were carried out on a modular air flow bench (AF10) experimental setup using a 27 cm long brass flat plate. The air flow bench consists of a small scale wind tunnel with adjustable airflow control and an electric fan. A flattened Pitot tube measures the total pressure at various distances from the plate surface by positioning the Pitot tube using a micrometer. The results are obtained by connecting the Pitot tube to the Setra brand model 239 pressure transducer. In addition, vortex generator experiments were carried out using the hot wire measurement method.

Experiments were carried out for 10 different ratios in the range of vortex generator height divided by boundary layer thickness, that is, the ratio h/δ, between 0.4 and 0.8. According to the results of the experiments for flow velocities 8,9,10,12 and 15 m/s without the vortex generator, it was determined that the flow in the boundary layer is laminar since the boundary layer thickness values found overlap with the Blasius solution in many locations. In addition, the results of the experiments without a vortex generator were confirmed by plotting the delta (δ)and Re graphs. It was determined that the positive pressure gradient effect increased the boundary layer thickness in

the experiments. It was also found that this effect makes the flow turbulent faster in experiments with vortex generators.

After positioning the vortex generators, it was determined that the flow of VGs kept the flow laminar for 4 or 5 cm and then the flow transitioned. In addition, it was determined in the experiments performed with vortex generators that the flow transition region length is decreased by VGs. Finally, where the vortex generators will be placed on the plate is a very important issue which determines transition onset and transition length.

4.1 Future Work

In this thesis, the effect of vortex generators on the boundary layer flow was investigated experimentally. The results can be supported by numerically analyzing the boundary layer flow in which the vortex generators used in the experiments are placed.

In this study, the vortex generators used spherical flat plate type vortex makers. Wheeler wishbone (Wishbone), Wheeler double (Doublet), backward-facing ramp and wedge type swirl makers in Lin (1999) and Lin (2002) were not used [6] [12]. In future studies, it can be experimentally examined how these types in the literature affect the transition in the boundary layer.

In the experiments, a flat plate of 27 cm was used and therefore it was necessary to work at low speeds to see the transition in the boundary layer. High Reynolds numbers can also be studied if studied in a more suitable experimental setup and on a longer flat plate.

REFERENCES

[1] Boundary layer: Definition characteristics, *Nuclear Power*, (2021, October 24), https://www.nuclear-power.com/nuclear-engineering/fluid-dynamics/boundary-layer/.

[2] **Canyurt, T.G.** (2016, June 29). Gemi Kıçındaki Akım Ayrılmasının Girdap Yapıcılar Aracılığıyla Kontrolü, *İTÜ Akademik Açık Arşiv: Home*, https://polen.itu.edu.tr/handle/11527/13533.

[3] **TANI, I. and KOMODA, H.** (1962). Boundary-layer transition in the presence of Streamwise Vortices, *Journal of the Aerospace Sciences*, *29*(4), 440 – 444.

[4] **Bakchinov, A.A.**, **Grek, G.R.**, **Klingmann, B.G. and Kozlov, V.V.** (1995). Transition experiments in a boundary layer with embedded streamwise vortices, *Physics of Fluids*, *7*(4), 820 – 832.

[5] **Singh, N.K.** (2019). Numerical simulation of flow behind Vortex Generators., *Journal of Applied Fluid Mechanics*, *12*(4), 1047 – 1061.

[6] **Lin, J.** (1999). Control of Turbulent Boundary Layer Separation Using Micro-Vortex Generators, *30th AIAA Fluid Dynamics Conference*, A99–33593, norfolk, VA.

[7] **Shahinfar, S.**, **Fransson, J.H.**, **Sattarzadeh, S.S. and Talamelli, A.** (2013). Scaling of streamwise boundary layer streaks and their ability to reduce skin-friction drag, *Journal of Fluid Mechanics*, *733*, 1–32.

[8] **Markland, E.** (1976). A first course in Air Flow, *Tecquipment*.

[9] **Bruun, H.** (1995). Hot-Wire Anemometry: Principles and Signal Analysis, *Oxford University Press, Oxford*.

[10] **Gad-el Hak, M. and Bushnell, D.** (1991). Separation control: Review, *Journal of Fluids Engineering*, *113*, 5 – 30.

[11] **Shahinfar, S.**, **Sattarzadeh, S.S.**, **Fransson, J.H. and Talamelli, A.** (2012). Revival of classical vortex generators now for transition delay, *Physical Review Letters*, *109*(7).

[12] **Lin, J.** (2002). Review of research on low-profile vortex generators to control boundary-layer separation, *Progress in Aerospace Sciences*, *38*(4-5), 389 – 420.

[13] **Shim, H. J., J.Y.H.**, **Chang, K.**, **Kwon, K.J. and Park, S.O.** (2015). Wake characteristics of vane-type vortex generators in a flat plate laminar boundary layer, *International Journal of Aeronautical and Space Sciences*, *16*(3), 325 – 338.

[14] **Urkiola, A.**, **Fernandez-Gamiz, U.**, **Errasti, I. and Zulueta, E.** (2017). Computational characterization of the Vortex generated by a vortex generator on a flat plate for different vane angles, *Aerospace Science and Technology*, *65*, 18 – 25.

[15] **Li, T.**, **Liang, H.**, **Zhang, J. and Zhang, J.** (2023). Numerical study on aerodynamic resistance reduction of high-speed train using vortex generator, *Engineering Applications of Computational Fluid Mechanics*, *17:1*, e2153925.

[16] **Siconolfi, L.**, **Camarri, S. and Fransson, J.H.** (2015). Stability analysis of boundary layers controlled by miniature vortex generators, *Journal of Fluid Mechanics*, *784*, 596–618.

[17] **Fransson, J.H.M.** (2015). Transition to turbulence delay using a passive flow control strategy, *Procedia IUTAM*, *14*, 385–393.

[18] **Paredes, P. and Choudhari, M. M., .L.F.** (2018). Transition delay via vortex generators in a hypersonic boundary layer at flight conditions, *2018 Fluid Dynamics Conference*.

[19] **Younes, E.**, **Hamidouche, S.**, **Gautier, R. and Russeil, S.** (2023). Spectral analysis of the transition to turbulence downstream a delta winglet pair vortex generator in an airflow channel, *Physics of Fluids*, *35*(1), 014108.

[20] **MATSUBARA, M. and ALFREDSSON, P.H.** (2001). Disturbance growth in boundary layers subjected to free-stream turbulence, *Journal of Fluid Mechanics*, *430*, 149–168.

[21] **Admin.** (n.d.). Model 239, *Test and Measurement Pressure Transducer*, `https://cdn2.hubspot.net/hubfs/211498/Setra_Product_Data_Sheets/Setra_Model_239_Data_Sheet.pdf`.

[22] **Başel, A.** (2013, June 11). İTÜ Trisonik Laboratuarı Aeorodinamik Deney Sonuçlarının Analizi ve görselleştirilmesi, *İTÜ Akademik Açık Arşiv: Home*, `https://polen.itu.edu.tr/items/ce94813f-dc75-4919-8a4e-df1c6ee780f2`.

APPENDICES

CURRICULUM VITAE

Name SURNAME: İsmet Cihat AY

EDUCATION:

- **B.Sc.:** 2019, University of Turkish Aeronautical Association, Faculty of Aeronautics and Astronautics, Aeronautical Engineering
- **M.Sc.:** Graduation year, University, Faculty, Department

PROFESSIONAL EXPERIENCE AND REWARDS:

- 2021-2022 AYD Automotive Industry

PUBLICATIONS, PRESENTATIONS AND PATENTS ON THE THESIS:

- Ay İ. C., Erdem D., (2023). Experimental Investigation of Boundary Layer Transition Via Vortex Generators. *2nd INTERNATIONAL GRADUATE RESEARCH SYMPOSIUM IGRS'23*, May 16-18, 2023 İstanbul, Turkey. (Presentation Instance)

OTHER PUBLICATIONS, PRESENTATIONS AND PATENTS: